**Supporting Information**

# Quantification of Nitrate-π Interactions and Selective Transport of Nitrate Using Calix[4]pyrroles with Two Aromatic Walls

Louis Adriaenssens,[†] Carolina Estarellas,[&] Andreas Vargas Jentzsch,[§] Marta Martinez Belmonte[†], Stefan Matile*[,§] and Pablo Ballester*[,†,‡]

[†] *Institute of Chemical Research of Catalonia (ICIQ), Avda. Països Catalans 16, 43007 Tarragona, Spain*

[&] *Department de Quimica, Universitat de les Illes Balears, ctra. Valldemossa km 7.5, E-07122, Palma de Mallorca, Spain*

[§] *Department of Organic Chemistry, University of Geneva, Geneva, Switzerland*

[‡] Catalan Institution of Research and Advanced Studies (ICREA), Passeig Lluís Companys 23, 08010 Barcelona, Spain

E-mail: pballester@iciq.es

**Contents**

# General Information and Instrumentation

Calixpyrroles **1**[1], **2c**[2], **2e**[3] and **3e**[3] were all prepared as described in the literature. Reagents were obtained from commercial suppliers and used without further purification unless otherwise stated. All solvents were commercially obtained and used without further purification except pyrrole which was distilled and then stored in the freezer for further use. Routine $^1$H NMR spectra were recorded on a Bruker Avance 300 (300 MHz for $^1$H NMR), Bruker Avance 400 (400 MHz for $^1$H NMR) or a Bruker Avance 500 (500 MHz for $^1$H NMR) ultrashield spectrometer. The deuterated solvents (Aldrich) used are indicated in the experimental part; chemical shifts are given in ppm. For $CDCl_3$ the peaks were referenced relative to the solvent residual peak $\delta$H = 7.26 ppm and $\delta$C = 77.0 ppm. For $CD_3CN$ the peaks were referenced relative to the solvent residual peak $\delta$H = 1.94 ppm. All NMR *J* values are given in Hz and are uncorrected. High resolution mass spectra were obtained on a Bruker Autoflex MALDI-TOF Mass Spectrometer. Mass spectra were recorded on a Waters LCT Premier ESI-TOF spectrometer, in an Agilent 1100 LC/MSD ESI-Quadrupole or in a Waters GTC spectrometer. Flash column chromatography was performed with Silica gel Scharlab60. Crystal structure determination was carried out using a Bruker-Nonius diffractometer equipped with a APPEX 2 4K CCD area detector, a FR591 rotating anode with MoK$\alpha$ radiation, Montel mirrors as monochromator and a Kryoflex low temperature device (T = 100 K). Full sphere data collection omega and phi scans. Programs used: Data collection Apex2 V. 1.0-22 (Bruker-Nonius 2004), data reduction Saint + Version 6.22 (Bruker-Nonius 2001) and absorption correction SADABS V. 2.10 (2003). Crystal structure solution was achieved using direct methods as implemented in SHELXTL Version 6.10 (Sheldrick, Universität Göttingen (Germany), 2000) and visualized using XP program. Missing atoms were subsequently located from difference Fourier synthesis and added to the atom list. Least-squares refinement on F2 using all measured intensities was carried out using the program SHELXTL Version 6.10 (Sheldrick, Universität Göttingen (Germany), 2000). Fluorescence measurements were performed with a FluoroMax-3 spectrofluorometer (Jobin-Yvon Spex) equipped with a stirrer and a temperature controller. All fluorescence measurements were performed at 25 °C.

# Synthesis

**General synthesis of dipyrromethanes S4a-e**

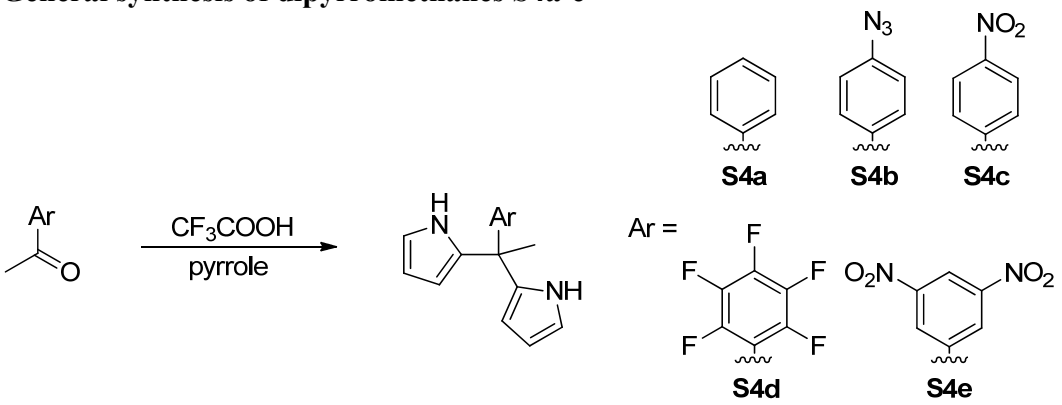


Trifluoroacetic acid (60 mmol, 3 equiv.) was added dropwise over 30 min to a stirred suspension or solution of the relevant acetophenone (20 mmol, 1 equiv) in pyrrole (30 mL, excess, 0.67 M soln.) cooled in an ice bath. The reaction was allowed to come to RT and stirred 14 h at RT. The reaction was diluted with water (10 mL) and basified to pH ≈ 10 with 2M $NaOH_{aq}$. During basification a cloudy precipitate forms. The reaction mixture is extracted with DCM. The organic extracts are combined, dried over $Na_2SO_4$, filtered and concentrated under vacuum. The resultant residue should be left for an extended period of time (several hours) under high vacuum so that as much pyrrole as possible is removed. If this thorough evaporation is not performed residual pyrrole will complicate the subsequent chromatography. The crude brown residue was subjected to column chromatography on silica (see below for specific conditions) and the first eluting fraction was collected.

**5-methyl-5-phenyl dipyrromethane S4a** (21% yield)

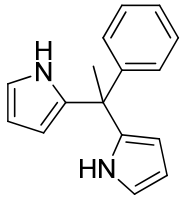


**purification**: silica chromatography (1:9 ethylacetate:hexane) followed by recrystallization from hexane.

**Rf** = 0.35 (1:9 ethylacetate:hexane, silica plate)

**$^1$H NMR** (400 MHz, $CDCl_3$, 25 ºC) δ (ppm) 2.06 (s, 3H), 5.98 (ddd, *J* = 3.4, 2.7, 1.5, 2H), 6.18 (dt, *J* = 3.4, 2.7, 2H), 6.68 (td, *J* = 2.6, 1.6, 2H), 7.10-7.15 (m, 2H), 7.21-7.32 (m, 3H), 7.78 (s, 2H)

**$^{13}$C{$^1$H} NMR** (75 MHz, $CDCl_3$, 25 ºC) δ (ppm) 28.8 ($CH_3$), 44.7 (C), 106.3 (CH), 108.2 (CH), 116.9 (CH), 126.7 (CH), 127.4 (CH), 128.1 (CH), 137.4 (C), 147.2 (C)

$^1$H NMR spectrum of this compound is in agreement with that reported in the literature.[4]

**5-methyl-5-(4′-azidophenyl) dipyrromethane S4b** (65% yield)

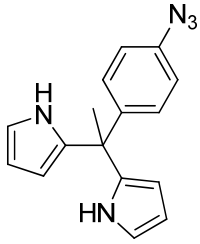


**purification**: silica chromatography (1:9 ethylacetate:)

**Rf** = 0.3 (1:9 ethylacetate:hexane, silica plate)

**$^1$H NMR** (400.1 MHz, $CDCl_3$) δ (ppm) 2.04 (s, 3H), 5.96 (ddd, *J* = 3.4, 2.7, 1.5, 2H), 6.18 (dt, *J* = 3.3, 2.6, 2H), 6.68 (td, *J* = 2.7, 1.5, 2H), 6.94 (d, *J* = 8.8, 2H), 7.10 (d, *J* = 8.8, 2H), 7.78 (broad s, 2H)

**$^{13}$C{$^1$H} NMR** (100.6 MHz, $CDCl_3$) δ (ppm) 28.78 (CH3), 44.37 (C), 106.40 (CH), 108.32 (CH), 117.09 (CH), 118.63 (CH), 128.85 (CH), 137.03 (C), 138.37 (C), 144.21 (C)

**5-methyl-5-(4´-nitrophenyl) dipyrromethane S4c** (48% yield)

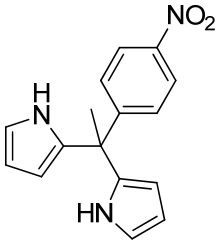

**purification**: silica chromatography (1:9 ethylacetate:hexane to 2:8 ethylacetate hexane)

**Rf** = 0.35 (2:8 ethylacetate:hexane, silica plate)

**$^{1}$H NMR** (400 MHz, $CDCl_3$, 25 ºC) δ (ppm) 2.10 (s, 3H), 5.96 (ddd, *J* = 3.4, 2.7, 1.5, 2H), 6.21 (dt, *J* = 3.4, 2.7, 2H), 6.75 (td, *J* = 2.7, 1.5, 2H), 7.29 (d, *J* = 8.9, 2H), 7.87 (s, 2H), 8.13 (d, *J* = 8.9, 2H)

**$^{13}$C{$^{1}$H} NMR** (75 MHz, $CDCl_3$, 25 ºC) δ (ppm) 28.5 ($CH_3$), 45.0 (C), 106.9 (CH), 108.5 (CH), 117.7 (CH), 123.2 (CH), 128.4 (CH), 135.7 (C), 146.6 (C), 155.0 (C)

All the spectroscopic data of this compound are in agreement with those reported in the literature.[2]

**5-methyl-5-(2´ ,3´ ,4´ ,5´ ,6´-pentafluorophenyl) dipyrromethane S4d** (9% yield)

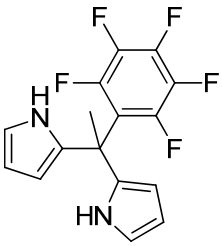

**purification**: silica chromatography (1:9 ethylacetate:hexane to 3:7 ethylacetate hexane)

**Rf** = 0.4 (16% ethylacetate in hexane, silica plate)

**$^{1}$H NMR** (300 MHz, $CDCl_3$, 25 ºC) δ (ppm) 2.23 (t, *J* = 2.5, 3H), 6.00 (ddd, *J* = 3.5, 2.7, 1.5, 2H), 6.16-6.20 (m, 2H), 6.70 (td, *J* = 2.7, 1.6, 2H), 7.99 (broad s, 2H)

**$^{13}$C{$^{1}$H} NMR** (75 MHz, $CDCl_3$, 25 ºC) δ (ppm) 28.1 (t, *J* = 5.2, $CH_3$), 42.2 (C), 105.9 (CH), 108.6 (CH), 117.4 (CH), 134.7 (C) (note that the signals for the carbon atoms of the pentafluorophenyl ring cannot be seen due to excessive splitting with the fluorine atoms)

**$^{19}$F{$^{1}$H} NMR** (375 MHz, $CDCl_3$, 25 ºC) δ (ppm) -137.11 to -137.24 (m, 2F), -156.20 (tt, *J* = 21.5, 2.9, 1F), -161.88 to -162.06 (m, 2F)

**5-methyl-5-(3´,5´-dinitrophenyl) dipyrromethane S4e** (51% yield)

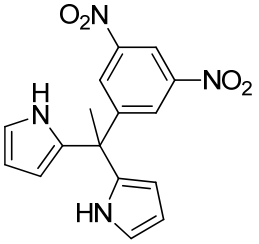

**purification**: silica chromatography (1:9 ethylacetate:hexane to 3:7 ethylacetate hexane)

**Rf** = 0.25 (2:8 ethylacetate:hexane, silica plate)

**$^{1}$H NMR** (500 MHz, $CDCl_3$, 25 ºC) δ (ppm) 2.14 (s, 3H), 5.90 (ddd, *J* = 3.5, 2.7, 1.5, 2H), 6.22 (dt, *J* = 3.5, 2.7, 2H), 6.78 (td, *J* = 2.7, 1.5, 2H), 7.94 (s, 2H), 8.31 (d, *J* = 2.1, 2H), 8.92 (t, *J* = 2.1, 1H)

**$^{13}$C{$^{1}$H} NMR** (75 MHz, $CDCl_3$, 25 ºC) δ (ppm) 28.4 ($CH_3$), 45.2 (C), 107.5 (CH), 109.0 (CH), 117.3 (CH), 118.5 (CH), 127.5 (CH), 134.3 (C), 148.3 (C), 152.7 (C)

All the spectroscopic data of this compound are in agreement with those reported in the literature.[3]

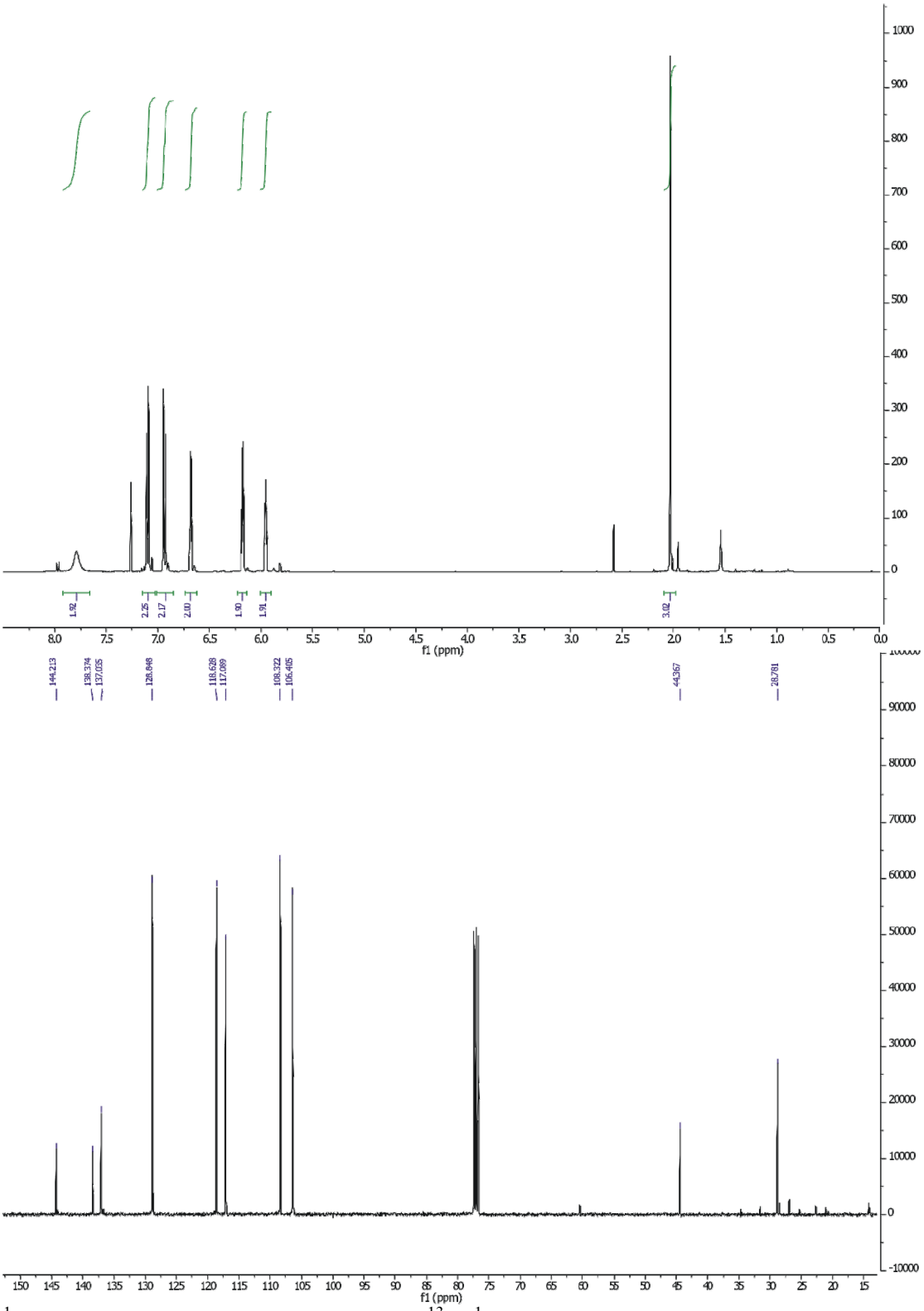


$^{1}$H-NMR (300 MHz, $CDCl_3$, 25 ºC) and $^{13}C\{^{1}H\}$ NMR (75 MHz, $CDCl_3$, 25 ºC) spectra of 5-methyl-5-(4´-azidophenyl) dipyrromethane **S4b**

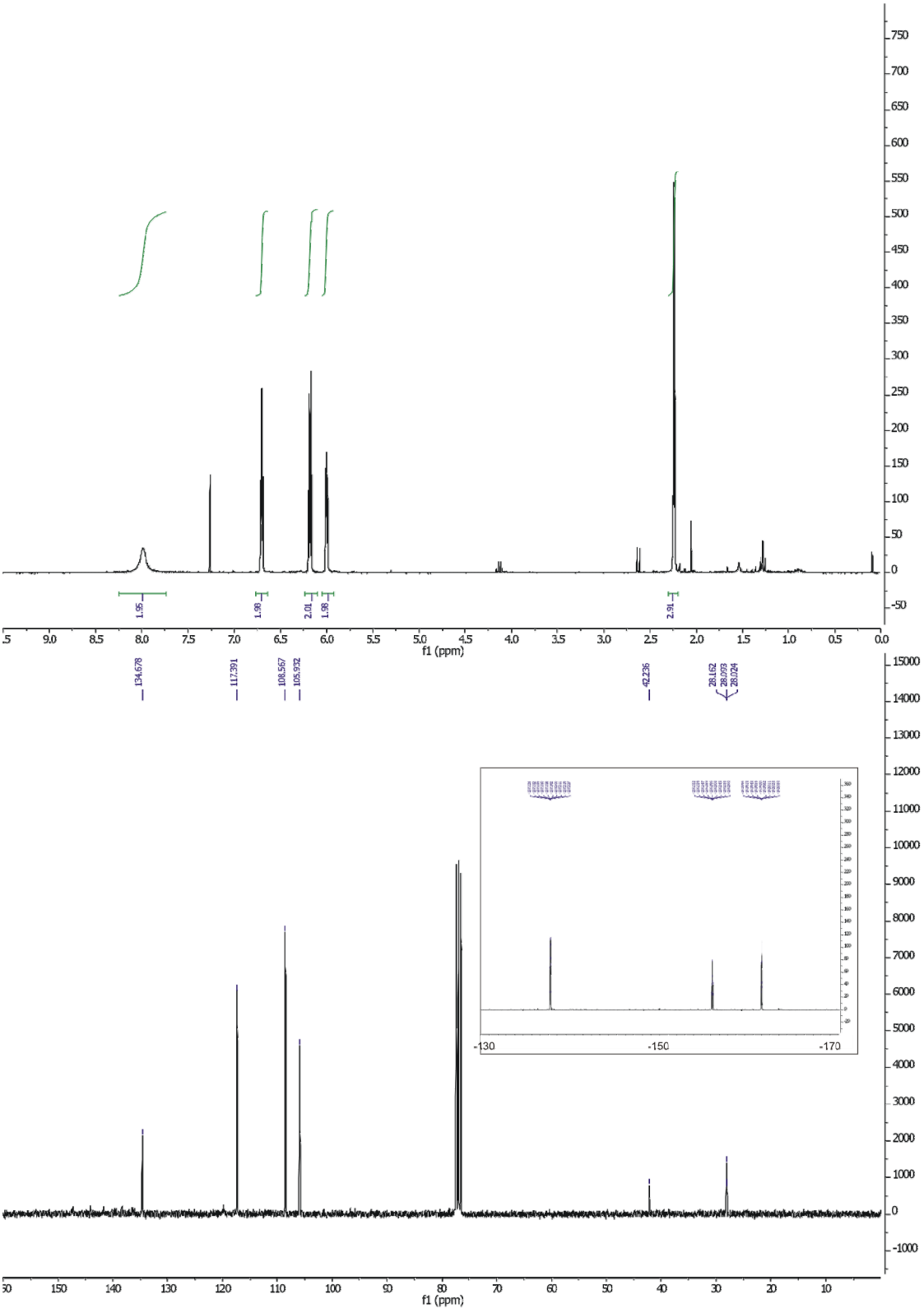


$^{1}$H-NMR (300 MHz), $^{13}$C{$^{1}$H} NMR (75 MHz) and $^{19}$F{$^{1}$H} NMR (375 MHz), $CDCl_3$, 25 ºC spectra of 5-methyl-5-(2´ ,3´ ,4´ ,5´ ,6´-pentafluorophenyl) dipyrromethane **S4d**

**Synthesis of α,α calix[4]pyrrole 2a.**

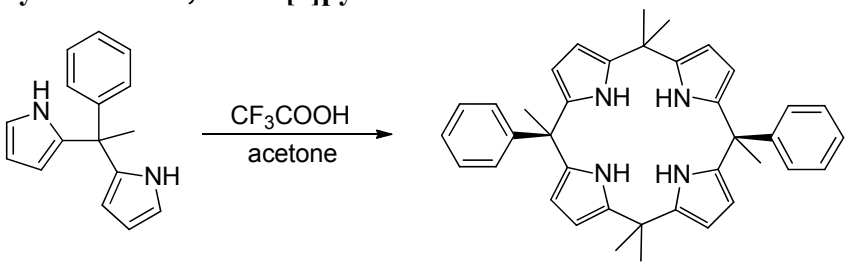


Trifluoroacetic acid (3.44 mL 45 mmol, 10 equiv.) was added dropwise to a solution of dipyrromethane **S4a** (1.00 g; 4.5 mmol, 1 equiv.) in acetone (HPLC grade, 30 mL) under argon atmosphere cooled in an ice bath. The mixture was allowed to come to RT and stirred for 14 hours. The reaction mixture was diluted with water (30 mL) and basified to pH ≈ 10 with 2M $NaOH_{aq}$. During basification the reaction mixture turned cloudy. The reaction mixture was extracted with DCM (3×). The DCM extracts were combined, dried over $Na_2SO_4$, filtered and evaporated to give a dark brown colored residue. This residue was purified on Silica (100% hexane to 1:9 ethyl acetate:hexane) and the second eluting fraction was collected to give α,α calixpyrrole **2a**. This was recrystallized from hot acetonitrile to give pure α,α calixpyrrole **2a** (60 mg, 5%).

α,α-calixpyrrole **2a**

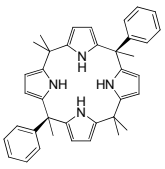

**Rf** = 0.40 (1:9 ethylacetate:hexane, silica plate)
**$^1$H-NMR** (300 MHz, $CDCl_3$, 25 ºC) δ (ppm) 1.54 (s, 6H), 1.62 (s, 6H), 1.90 (s, 6H), 5.63 (t, *J* = 3.0, 4H), 5.92 (t, *J* = 3.0, 4H), 6.94-7.02 (m, 4H), 7.16-7.30 (m, 10H)
**$^{13}$C{$^1$H} NMR** (75 MHz, $CDCl_3$, 25 ºC) δ (ppm) 27.8 ($CH_3$), 27.9 ($CH_3$), 30.0 ($CH_3$), 35.1 (C), 44.7 (C), 103.1 (CH), 105.9 (CH), 126.3 (CH), 127.4 (CH), 127.6 (CH), 136.6 (C), 138.4 (C), 147.9 (C)
**HR-MS** (ESI+ve) m/z calcd for $C_{38}H_{41}N_4$ ($[M+H]^+$) 553.3331, found 553.3346.
**IR** $\tilde{\nu}$ ($cm^{-1}$) 1038 s; 1278 s; 2966 s; 3400 s; 3411 s; 3478 m
**m.p.** 245 °C (decomposition).

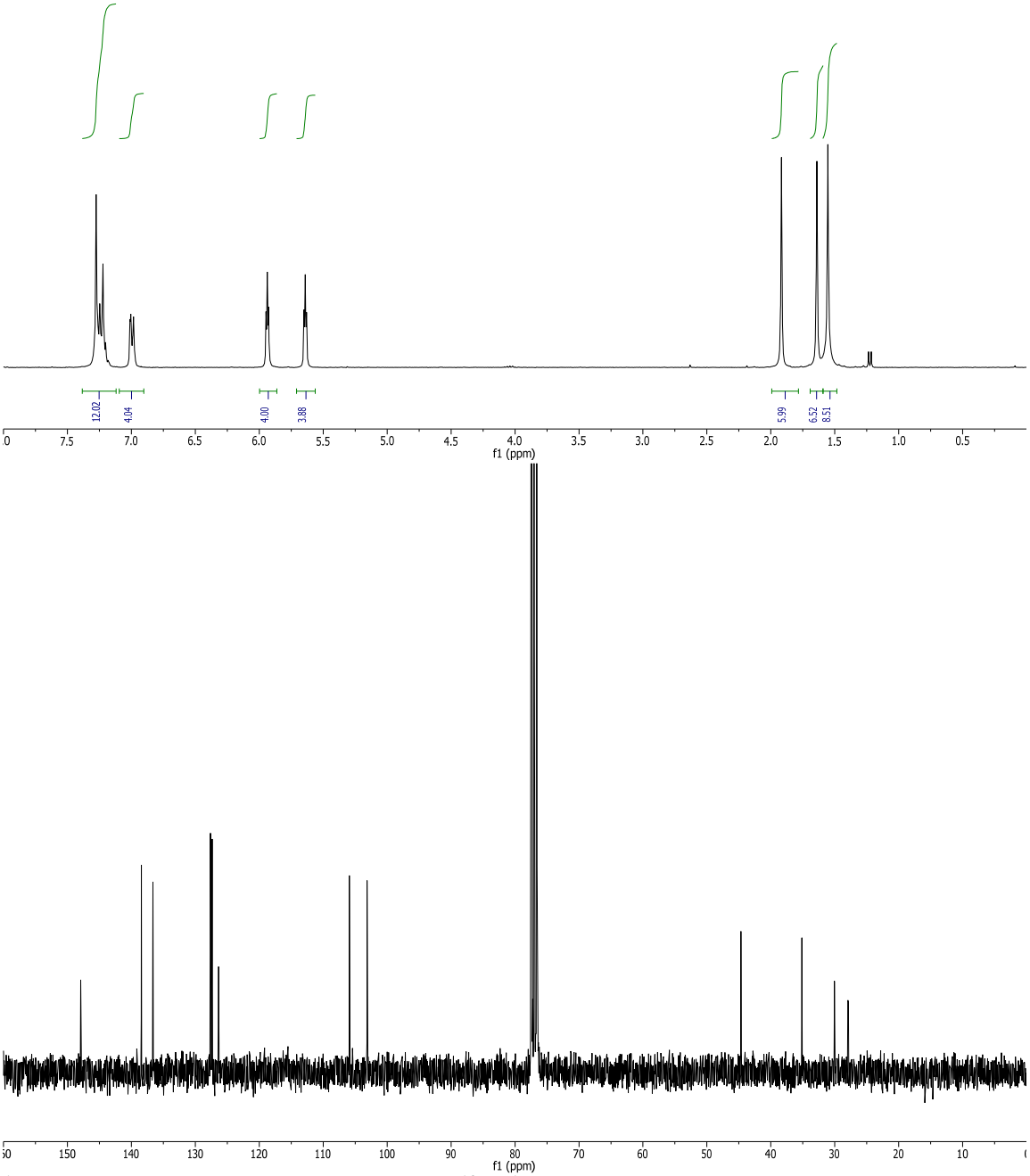


$^{1}$H-NMR (300 MHz, $CDCl_3$, 25 ºC) and $^{13}C\{^{1}H\}$ NMR (75 MHz, $CDCl_3$, 25 ºC) spectra of **2a**.

**Synthesis of α,α calix[4]pyrrole 2b.**

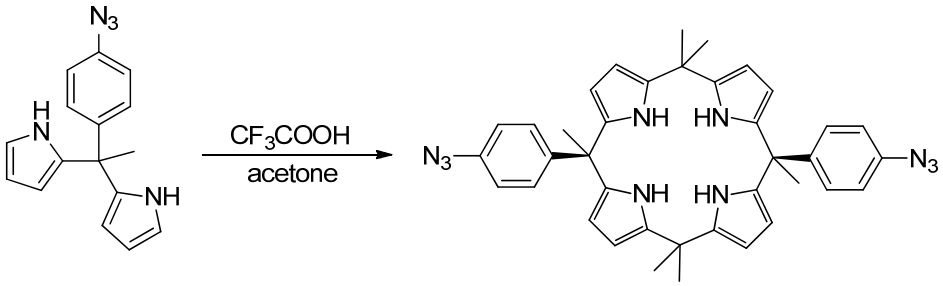


Trifluoroacetic acid (4.22 mL 55 mmol, 10 equiv.) was added dropwise to a solution of dipyrromethane **S4b** (1.53 g; 5.5 mmol, 1 equiv.) in acetone (HPLC grade, 37 mL) under argon atmosphere cooled in an ice bath. The mixture was allowed to come to RT and stirred for 14 hours. The reaction mixture was diluted with water (100 mL) and basified to pH ≈ 10 with 2M $NaOH_{aq}$. The reaction mixture was extracted with DCM (3×). The DCM extracts were combined, dried over $Na_2SO_4$, filtered and evaporated to give a dark brown colored residue. This residue was purified on Silica (100% hexane to 3:17 ethyl acetate:hexane) and the second eluting fraction was collected to give α,α calixpyrrole **2a** (184 mg, 10.5%).

α,α-calixpyrrole **2b**

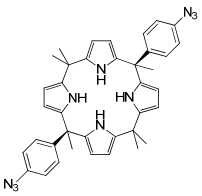


**Rf** = 0.37 (1:9 ethylacetate:hexane, silica plate)
**$^1$H-NMR** (300 MHz, $CDCl_3$, 25 ºC) δ (ppm) 1.54 (s, 6H), 1.62 (s, 6H), 1.88 (s, 6H), 5.62 (t, *J* = 3.0, 4H), 5.93 (t, *J* = 3.0, 4H), 6.89 (d, *J* = 8.7, 4H), 6.96 (d, *J* = 8.7, 4H), 7.19 (broad s, 4H)
**$^{13}$C{$^1$H} NMR** (75 MHz, $CDCl_3$, 25 ºC) δ (ppm) 27.7 ($CH_3$), 27.8 ($CH_3$), 30.1 ($CH_3$), 35.1 (C), 44.3 (C), 103.3 (CH), 106.0 (CH), 118.2 (CH), 128.8 (CH), 136.2 (CH), 138.1 (C), 138.5 (C), 144.9 (C)
**HR-MS** (ESI+ve) m/z calcd for $C_{38}H_{39}N_{10}$ ($[M+H]^+$) 635.3354, found 635.3386.
**IR** $\tilde{\nu}$ ($cm^{-1}$) 1036 s; 1268 s; 1499 s, 2115 s, 2972 m; 3420 m; 3442 m
**m.p.** 195 °C (decomposition).

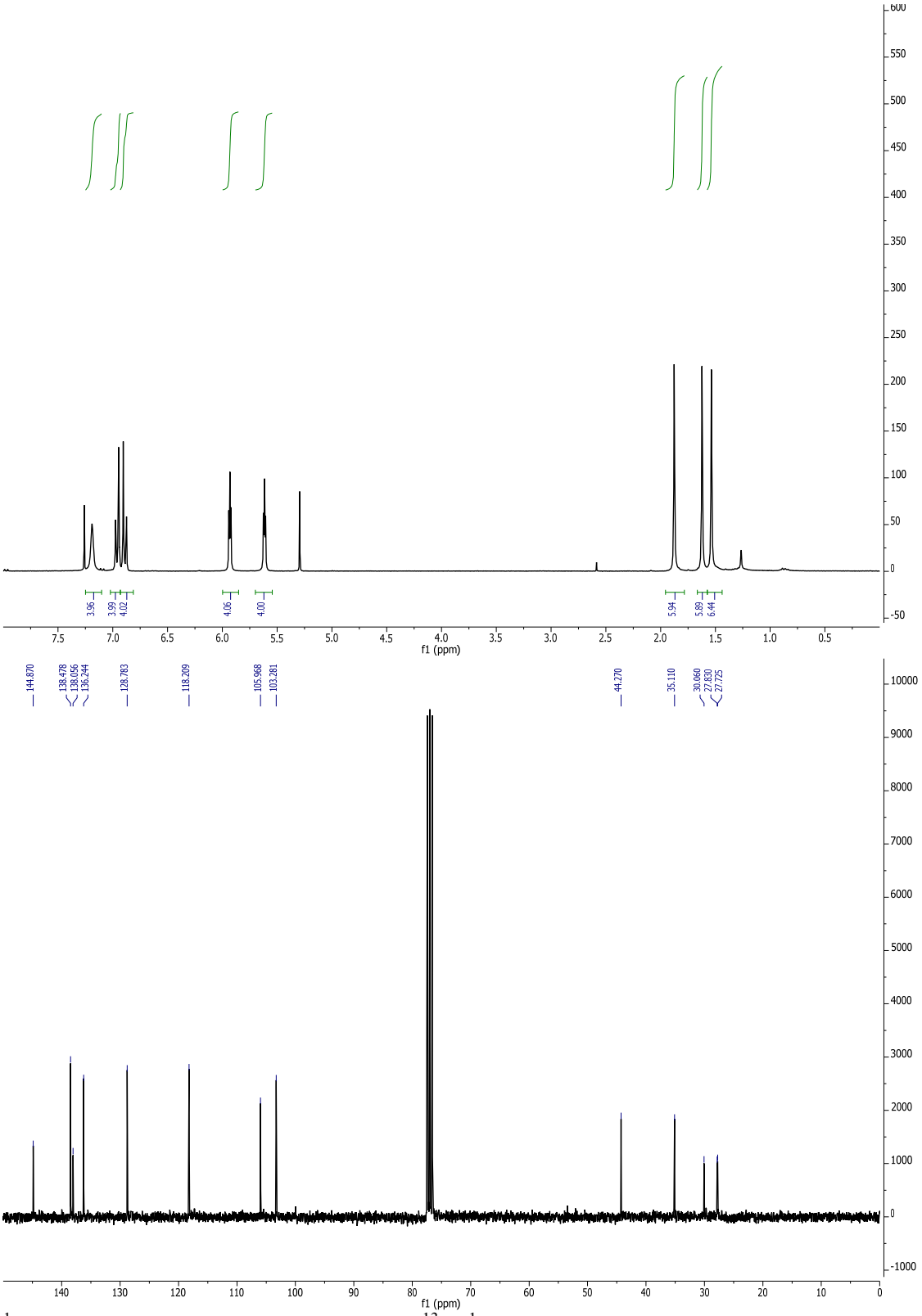


$^{1}$H-NMR (300 MHz, $CDCl_3$, 25 ºC) and $^{13}C\{^{1}H\}$ NMR (75 MHz, $CDCl_3$, 25 ºC) spectra of **2b**.

**Synthesis of α,α calix[4]pyrrole 2c.**

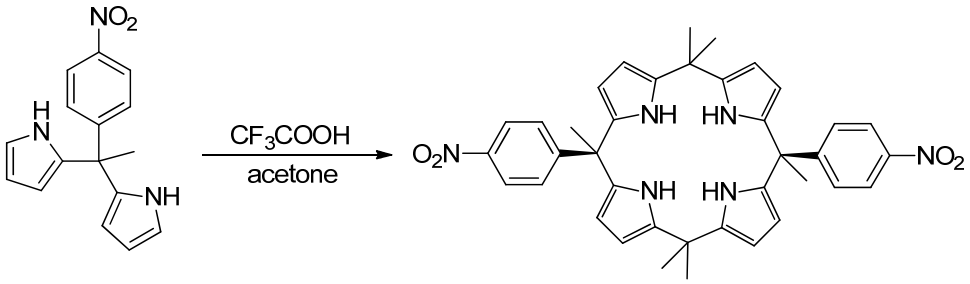


Trifluoroacetic acid (3.35 mL 43.8 mmol, 10 equiv.) was added dropwise to a solution of dipyrromethane **S4c** (1.17 g; 4.38 mmol, 1 equiv.) in acetone (HPLC grade, 29 mL) under argon atmosphere cooled in an ice bath. The mixture was allowed to come to RT and stirred for 14 hours. The reaction mixture was diluted with water (30 mL) and basified to pH ≈ 10 with 2M $NaOH_{aq}$. During basification the reaction mixture turned cloudy. The reaction mixture was extracted with DCM (3×). The DCM extracts were combined, dried over $Na_2SO_4$, filtered and evaporated to give a dark red colored residue. This residue was purified on Silica (100% hexane to 3:7 ethyl acetate:hexane) and the second eluting fraction was collected to give α,α calixpyrrole **2c**. This was recrystallized from hot isopropanol to give pure α,α **2c** (99.5 mg, 7%).

α,α-calixpyrrole **2c**

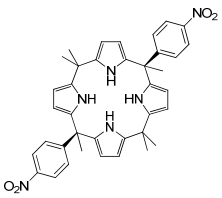


**Rf** = 0.32 (2:8 ethylacetate:hexane, silica plate)
**$^1$H-NMR** (300 MHz, $CDCl_3$, 25 ºC) δ (ppm) 1.56 (s, 6H), 1.65 (s, 6H), 1.93 (s, 6H), 5.62 (t, *J* = 3.1, 4H), 5.98 (t, *J* = 3.0, 4H), 7.16 (d, *J* = 8.9, 4H), 7.23 (s, 4H), 8.10 (d, *J* = 8.8, 4H)
**$^{13}$C{$^1$H} NMR** (75 MHz, $CDCl_3$, 25 ºC) δ (ppm) 27.5 ($CH_3$), 27.8 ($CH_3$), 30.0 ($CH_3$), 35.2 (C), 45.0 (C), 103.6 (CH), 106.4 (CH), 122.9 (CH), 128.4 (CH), 135.1 (C), 138.8 (C), 146.6 (C), 155.3 (C)

All the spectroscopic data of this compound is in agreement with that reported in the literature.[2]

**Synthesis of calix[4]pyrroles 2d and 3d.**

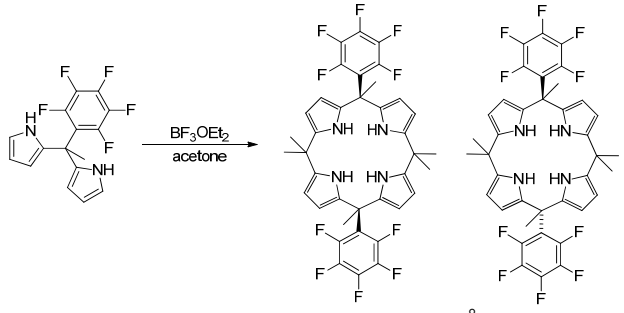


(Acetone that has been stored over 4Å molecular sieves for one night is used for this synthesis. It is passed through a syringe tip filter during addition to eliminate any particles of molecular sieves.)

$BF_3OEt_2$ (75 μL, 0.59 mmol, 1.1 equiv.) is added dropwise to a stirred solution of dipyromethane **S4d** (174.6 mg, 0.535 mmol, 1 equiv.) in acetone (13 mL) under Ar. The reaction stirs for 3 hours at RT and is then diluted with water (13 mL). The reaction mixture is evaporated under vacuum until it is judged that most of the acetone has been removed. The reaction mixture is basified to pH ≈ 10 with $NaOH_{aq}$ (2M) and extracted with DCM (3×). The DCM extracts are combined, dried over $Na_2SO_4$, filtered and evaporated in vacuo. The resultant residue is purified on silica (2:8 ethylacetate:hexane to 4:6 ethylacetate:hexane). The first fraction to elute is α,β **3d**, the second is α,α **2d**. The two fractions are collected separately to give pure α,β **3d** (44.0mg, 22%) as a pale yellow solid and pure α,α **2d** as a white solid (45.2 mg, 23%)

α,α-calixpyrrole **2d**

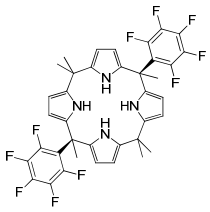

**Rf** = 0.55 (2:8 ethylacetate:hexane, silica plate)

**$^1$H-NMR** (300 MHz, $CDCl_3$, 25 ºC) δ (ppm) 1.52 (s, 6H), 1.60 (s, 6H), 2.10 (broad s, 6H), 5.72 (t, *J* = 3.0, 4H), 5.95 (t, *J* = 3.0, 4H), 7.24 (broad s, 4H)

**$^{13}$C{$^1$H} NMR** (75 MHz, $CDCl_3$, 25 ºC) δ (ppm) 26.1 ($CH_3$), 27.8 ($CH_3$), 30.0 ($CH_3$), 35.2 (C), 41.7 (C), 103.7 (CH), 105.3 (CH), 133.6 (C), 138.7 (C) (note that the signals for several carbon atoms cannot be seen due to excessive splitting with the fluorine atoms)

**$^{19}$F{$^1$H} NMR** (375 MHz, $CDCl_3$, 25 ºC) δ (ppm) -137.74 (broad s, 4F), -156.6 (t, *J* = 21.4, 2F), -162.46 (td, *J* = 22.1, 6.7, 4F)

**HR-MS** (ESI+ve) m/z calcd for $C_{38}H_{31}N_4F_{10}$ ($[M+H]^+$) 733.2384, found 733.2378.

**IR** $\tilde{\nu}$ ($cm^{-1}$) 1274 m; 987 s, 1420 m; 1481 s, 1521 s, 1648 w, 2977 m, 3416 s

**m.p.** 290-292 °C (partial decomposition).

α,β-calixpyrrole **3d**

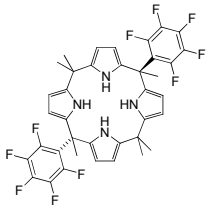

**Rf** = 0.7 (2:8 ethylacetate:hexane, silica plate)

**$^1$H-NMR** (300 MHz, $CDCl_3$, 25 ºC) δ (ppm) 1.54 (s, 12H), 2.13 (t, *J* = 2.6, 6H), 5.84 (t, *J* = 3.1, 4H), 5.97 (dd, *J* = 2.7, 3.4, 4H), 7.21 (broad s, 4H)

**$^{13}$C{$^1$H} NMR** (75 MHz, $CDCl_3$, 25 ºC) δ (ppm) 27.8 ($CH_3$), 29.3 ($CH_3$), 35.5 (C), 42.3 (C), 103.9 (CH), 105.4 (CH), 133.8 (C), 138.7 (C) (note

that the signals for several carbon atoms cannot be seen due to excessive splitting with the fluorine atoms)

**$^{19}F\{^{1}H\}$ NMR** (375 MHz, $CDCl_3$, 25 ºC) δ (ppm) -136.46 (broad d, *J* = 18.5, 4F), -156.3 (broad t, *J* = 21.4, 2F), -162.03 (td, *J* = 22.2, 6.5, 4F)

**HR-MS** (ESI+ve) m/z calcd for $C_{38}H_{31}N_4F_{10}$ ($[M+H]^+$) 733.2384, found 733.2397.

**IR** $\tilde{\nu}$ ($cm^{-1}$) 1277 m; 1475 s, 1520 s, 1648 w, 2972 m, 3423 m, 3450 m

**m.p.** 131-133 °C

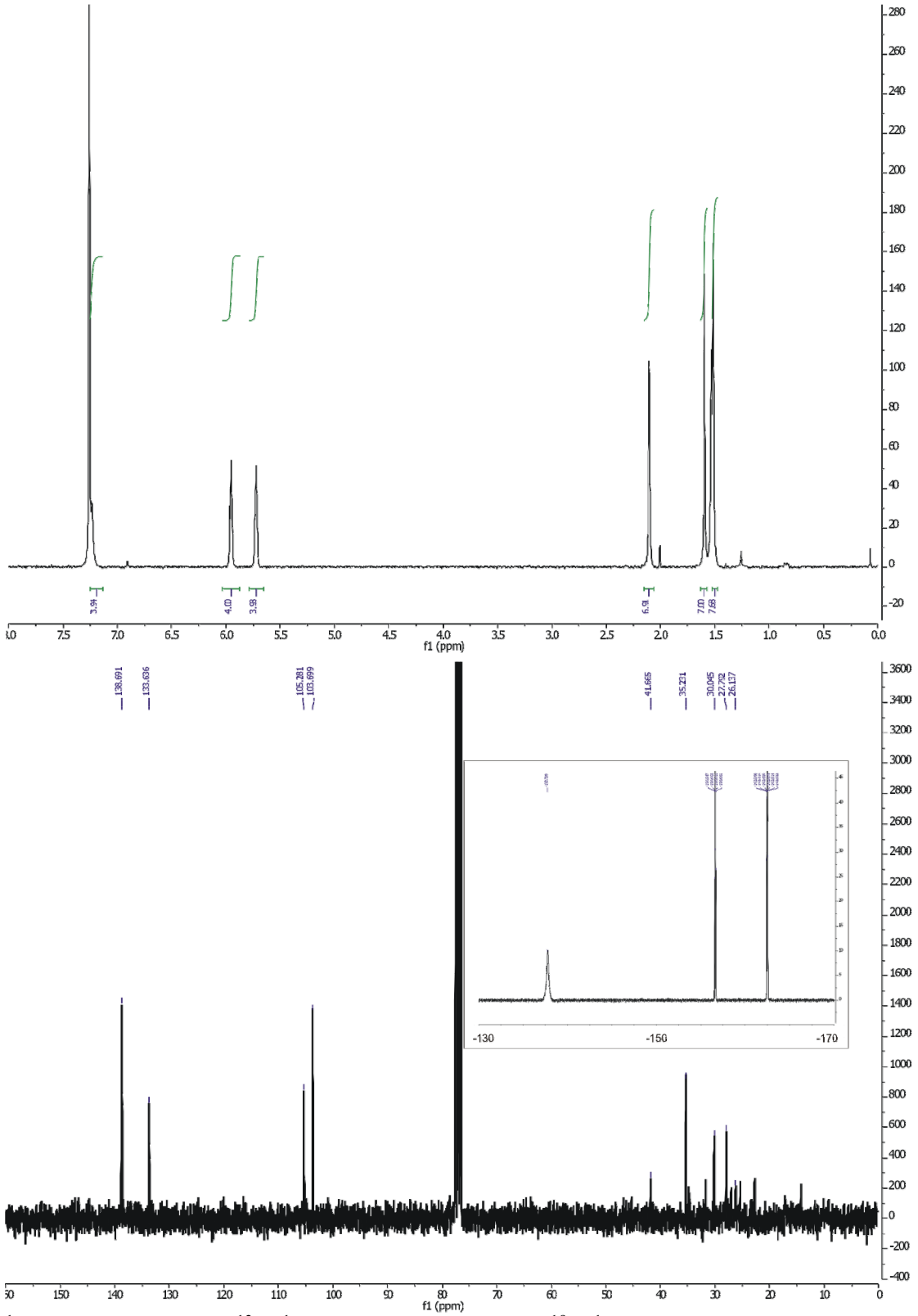


$^{1}$H-NMR (300 MHz), $^{13}$C{$^{1}$H} NMR (75 MHz) and $^{19}$F{$^{1}$H} NMR (375 MHz), $CDCl_3$, 25 ºC spectra of **2d**.

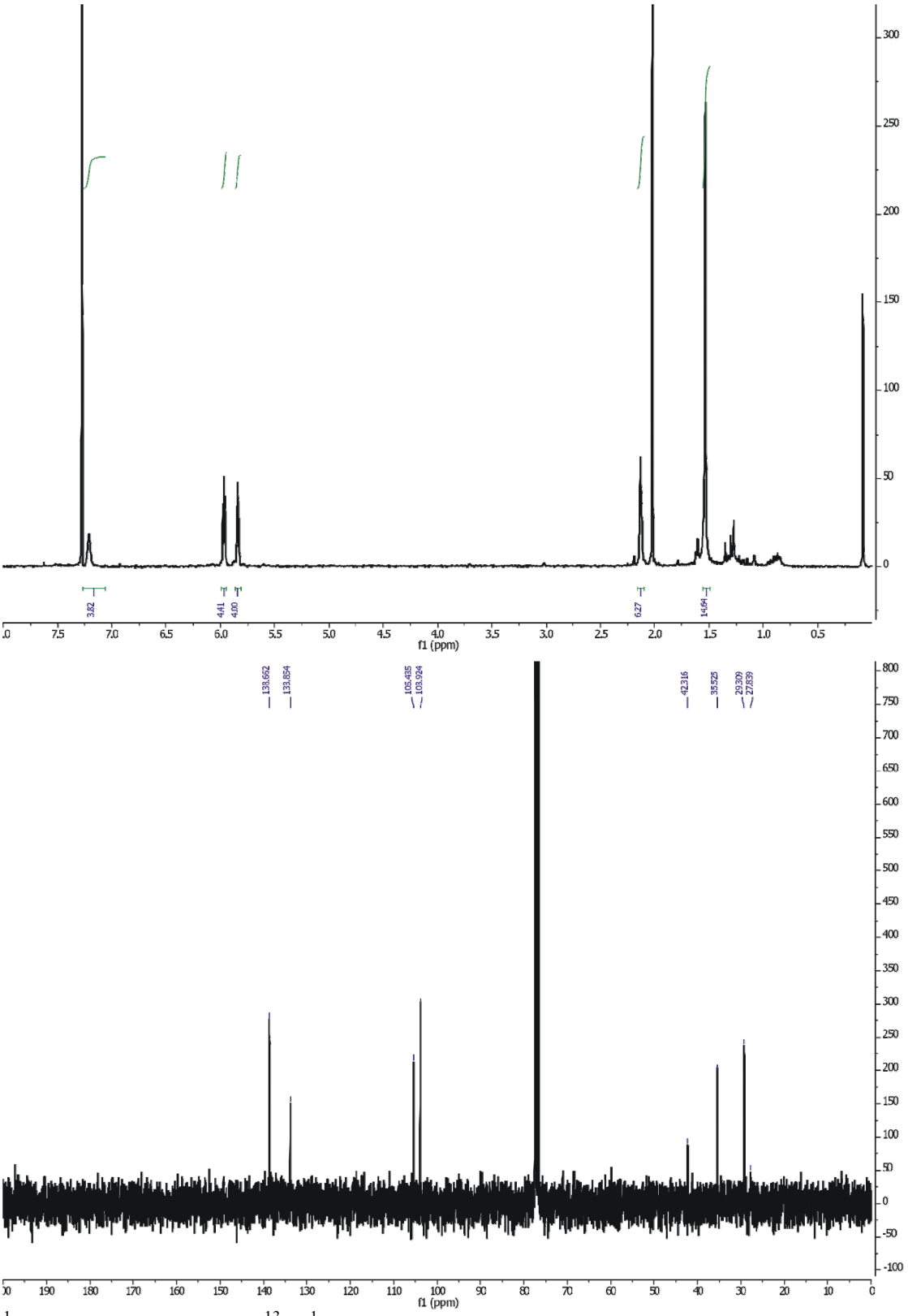


$^{1}$H-NMR (300 MHz) and $^{13}$C{$^{1}$H} NMR (75 MHz) $CDCl_3$, 25 ºC spectra of **3d**.

**Synthesis of calix[4]pyrroles 2e and 3e.**

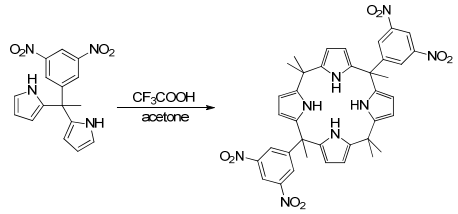


Trifluoroacetic acid (0.70 mL 9.2 mmol) was added dropwise to a solution of 3,5dinitrophenyl dipyrromethane **S4e** (0.30 g; 0.92 mmol) in acetone (HPLC grade, 6.5 mL) under argon atmosphere cooled in an ice bath. The mixture was stirred at room temperature for 14 hours during which time a red precipitate had formed in the reaction mixture. The reaction mixture was diluted with water (10 mL) and basified to pH ≈ 10 with 2M $NaOH_{aq}$. During basification the reaction mixture turned cloudy. The reaction mixture was extracted with DCM (3×). The DCM extracts were combined, dried over $Na_2SO_4$, filtered and evaporated to give a dark red colored residue. This residue was purified on Silica (1:19 ethyl acetate:hexane to 4:6 ethyl acetate:hexane) to yield both isomers of the calix[4]pyrrole. The first fraction to elute is the α,β isomer **3e** and the second eluting fraction is the α,α isomer **2e**. The two calixpyrroles were recrystallized from hot acetonitrile to give pure α,β **3e** (41.1 mg, 6%) and α,α **2e** (36.2 mg, 5%).

α,α-calixpyrrole **2e**

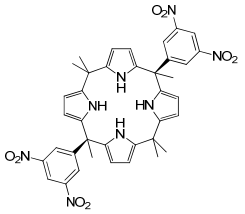


**Rf** = 0.18 (2:8 ethylacetate:hexane, silica plate)
**$^1$H-NMR** (400 MHz, $CDCl_3$, 25 ºC) δ (ppm) 1.60 (s, 6H), 1.68 (s, 6H), 2.01 (s, 6H), 5.59 (t, *J* = 3.2, 4H), 6.01 (t, *J* = 3.0, 4H), 7.28 (s, 4H), 8.17 (d, *J* = 2.1, 4H), 8.91 (t, *J* = 2.1, 2H)
**$^{13}$C{$^1$H} NMR** (75 MHz, $CDCl_3$, 25 ºC) δ (ppm) 27.1 ($CH_3$), 27.6 ($CH_3$), 30.0 ($CH_3$), 35.3 (C), 45.0 (C), 104.2 (CH), 106.9 (CH), 117.2 (CH), 127.5 (CH), 134.0 (C), 139.6 (C), 148.1 (C), 152.6 (C)

α,β-calixpyrrole **3e**

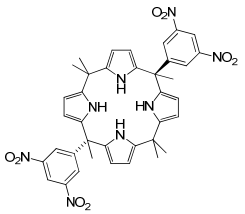


**Rf** = 0.25 (2:8 ethylacetate:hexane, silica plate)
**$^1$H-NMR** (300 MHz, $CDCl_3$, 25 ºC) δ (ppm) 1.62 (s, 12H), 2.01 (s, 6H), 5.71 (t, *J* = 3.1, 4H), 6.00 (t, *J* = 3.0, 4H), 7.42 (s, 4H), 8.31 (d, *J* = 2.1, 4H), 8.90 (t, *J* = 2.0, 2H)
**$^{13}$C{$^1$H} NMR** (75 MHz, $CDCl_3$, 25 ºC) δ (ppm) 29.0 ($CH_3$), 29.3 ($CH_3$), 35.6 (C), 45.0 (C), 104.1 (CH), 107.0 (CH), 117.2 (CH), 127.5 (CH), 134.0 (C), 140.1 (C), 148.2 (C), 151.5 (C)

All spectroscopic data for these compounds is in agreement with that reported in the literature.[3] The only notable difference lies in the number of protons assigned to the signal resonating at 8.91 ppm in the $^1$H NMR of compound **2e**. In the literature this signal has mistakenly been assigned 4 protons instead of 2 protons.

**Binding Studies - $^1$H NMR Titrations**

All titrations were carried out on a Bruker 500 MHz or 400 MHz spectrometer, at 298 K, in acetonitrile-$d_3$ ($CD_3CN$). For all receptors the complexation of $[Bu_4N]^+[NO_3]^-$ showed a fast exchange regime in the NMR timescale. The association constant between receptors **1** and **2a-e** and the nitrate anion was determined by monitoring the chemical shift changes of the proton signals corresponding to the receptors in the $^1$H NMR spectrum (and in the case of **2d** the $^{19}$F NMR spectrum as well) as incremental amounts of the guest were added. As many signals as possible were monitored but sometimes excessive broadening or peak overlap rendered a specific signal impossible to follow. The value of the association constant was calculated using the software HypNMR[5] which uses least-squares minimization to obtain globally optimized parameters. In all cases the data fit well to a simple 1:1 binding model.

Specifically, the association constants were determined using about 1-2 mM solutions of **1** and **2a-e** in $CD_3CN$ at 298 K, and adding aliquots of a solution of $[Bu_4N]^+[NO_3]^-$, approximately 20 or 30 times more concentrated, in the same solvent. In this manner, by using the afore mentioned 1-2 mM solutions of **1** and **2a-e** to prepare the solutions of $[Bu_4N]^+[NO_3]^-$ the concentration of the receptor was maintained constant throughout the titration. The association constant (Ka) for the binding process between receptors **1** and **2a-e** and the nitrate anion were determined by averaging the values from at least two titrations.

**Calixpyrrole 1 nitrate binding**

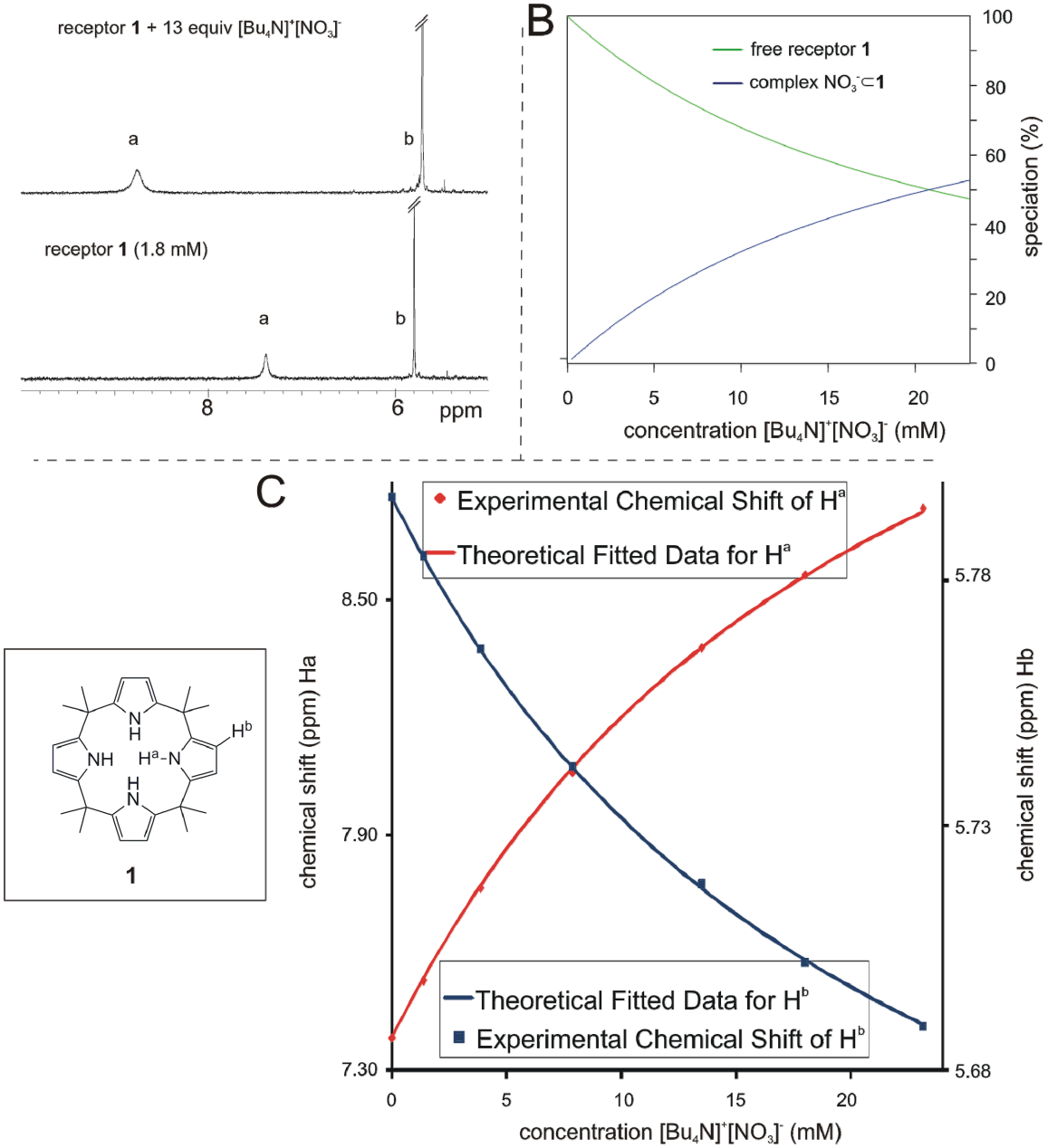


**Figure S 1** Binding data taken from the titration of calixpyrrole **1** with $[Bu_4N]^+[NO_3]^-$. panel A: $^1$H NMR (400 MHz, $CD_3CN$, 298 K) spectra of the starting point (1.8 mM **1**) and end point (1.8 mM **1** with 13 equiv $[Bu_4N]^+[NO_3]^-$) of the titration. Panel B: speciation of free calixpyrrole **1** and host guest complex $NO_3^-\subset$**1** as a function of $[Bu_4N]^+[NO_3]^-$ concentration. Panel C: fitting of the $^1$H NMR data

**Calixpyrrole 2a nitrate binding**

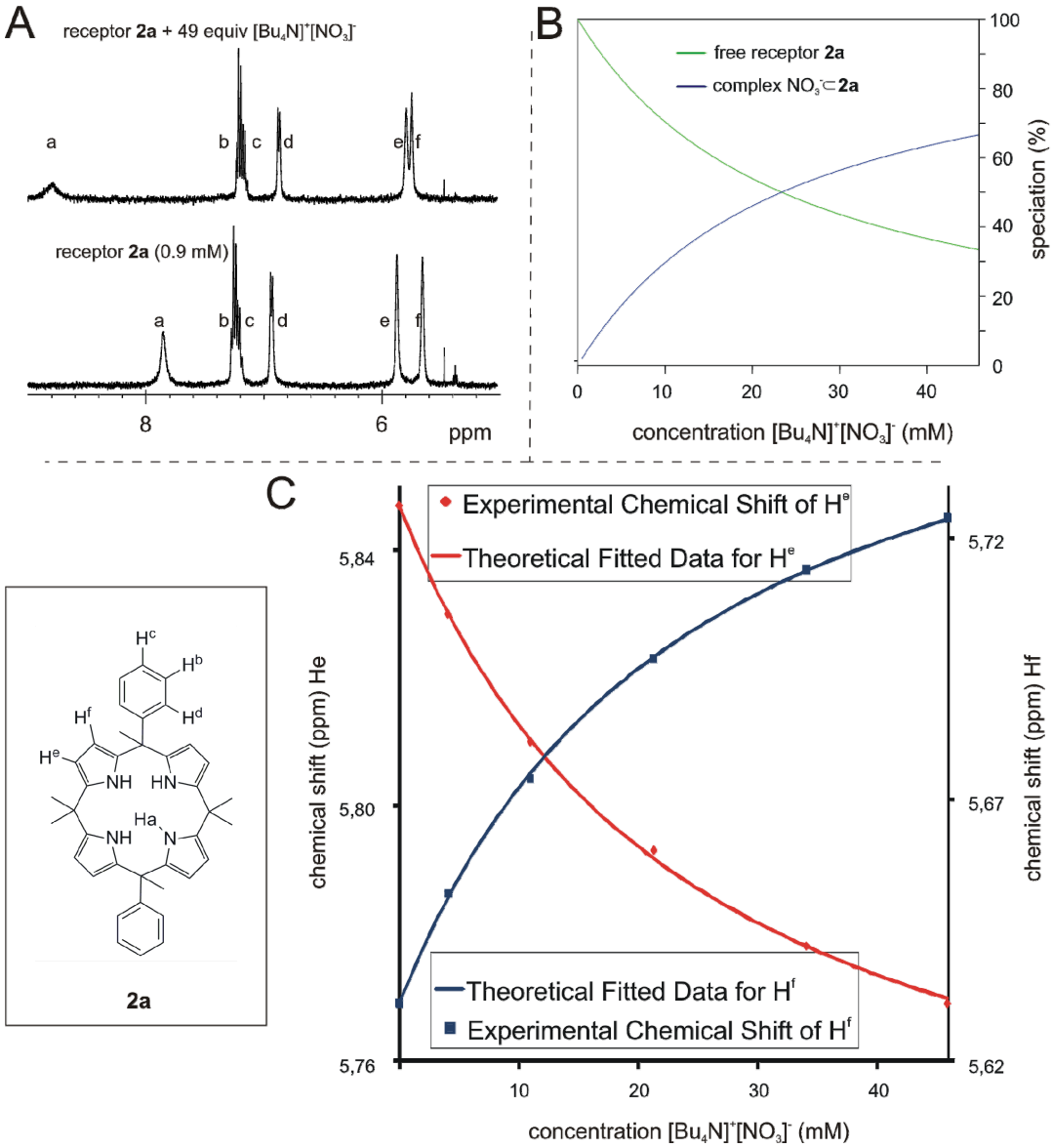


**Figure S 2** Binding data taken from the titration of calixpyrrole **2a** with $[Bu_4N]^+[NO_3]^-$. Panel A: $^1$H NMR (400 MHz, $CD_3CN$, 298 K) spectra of the starting point (0.91 mM **2a**) and end point (0.91 mM **2a** with 49 equiv $[Bu_4N]^+[NO_3]^-$) of the titration. Panel B: speciation of free calixpyrrole **2a** and host guest complex $NO_3^-\subset$**2a** as a function of $[Bu_4N]^+[NO_3]^-$ concentration. Panel C: fitting of the $^1$H NMR data

**Calixpyrrole 2b nitrate binding**

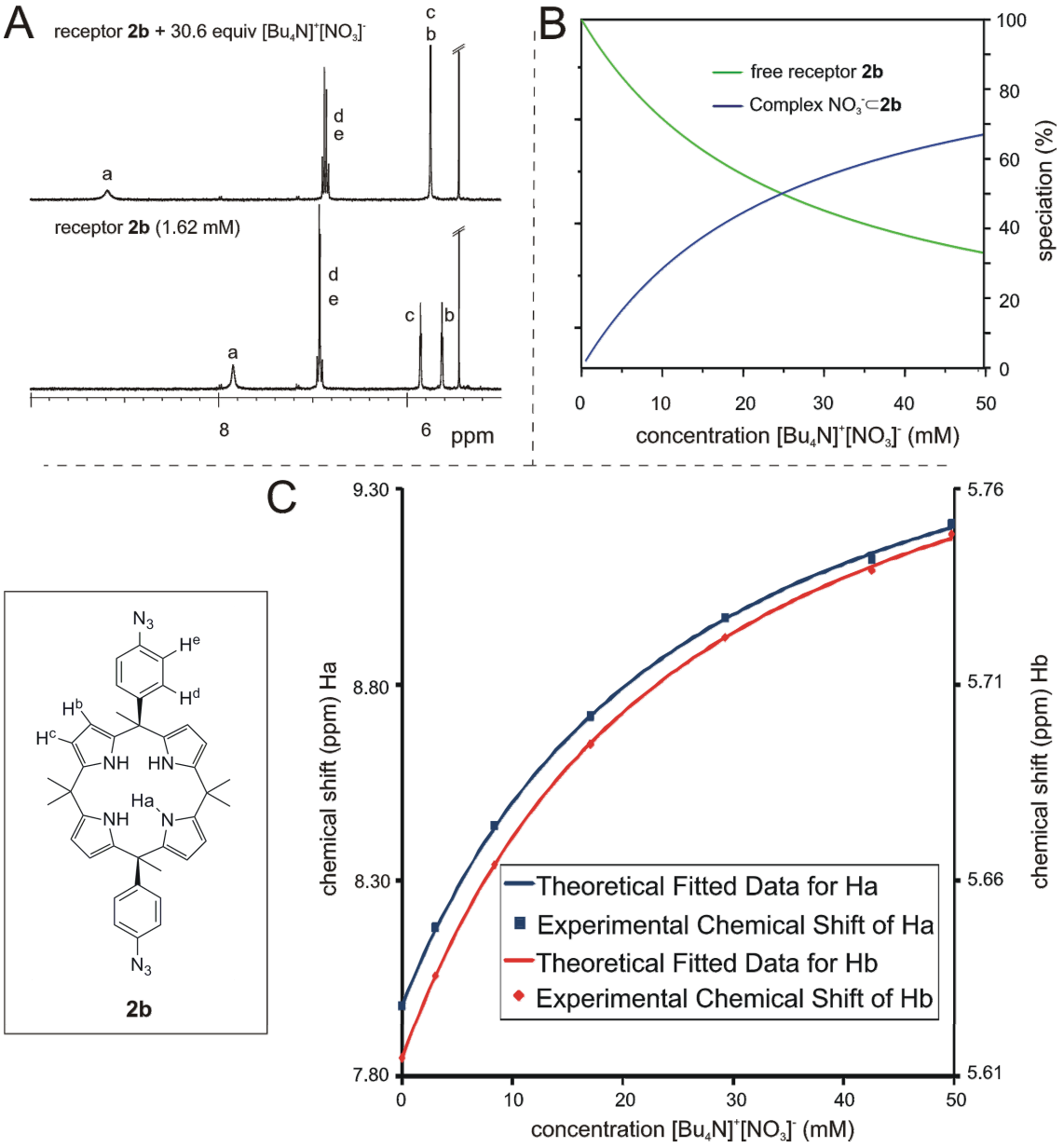


**Figure S 3** Binding data taken from the titration of calixpyrrole **2b** with $[Bu_4N]^+[NO_3]^-$. panel A: $^1$H NMR (400 MHz, $CD_3CN$, 298 K) spectra of the starting point (1.6 mM **2b**) and end point (1.6 mM **2b** with 30.6 equiv $[Bu_4N]^+[NO_3]^-$) of the titration. Panel B: speciation of free calixpyrrole **2b** and host guest complex $NO_3^-\subset$**2b** as a function of $[Bu_4N]^+[NO_3]^-$ concentration. Panel C: fitting of the $^1$H NMR data

**Calixpyrrole 2c nitrate binding**

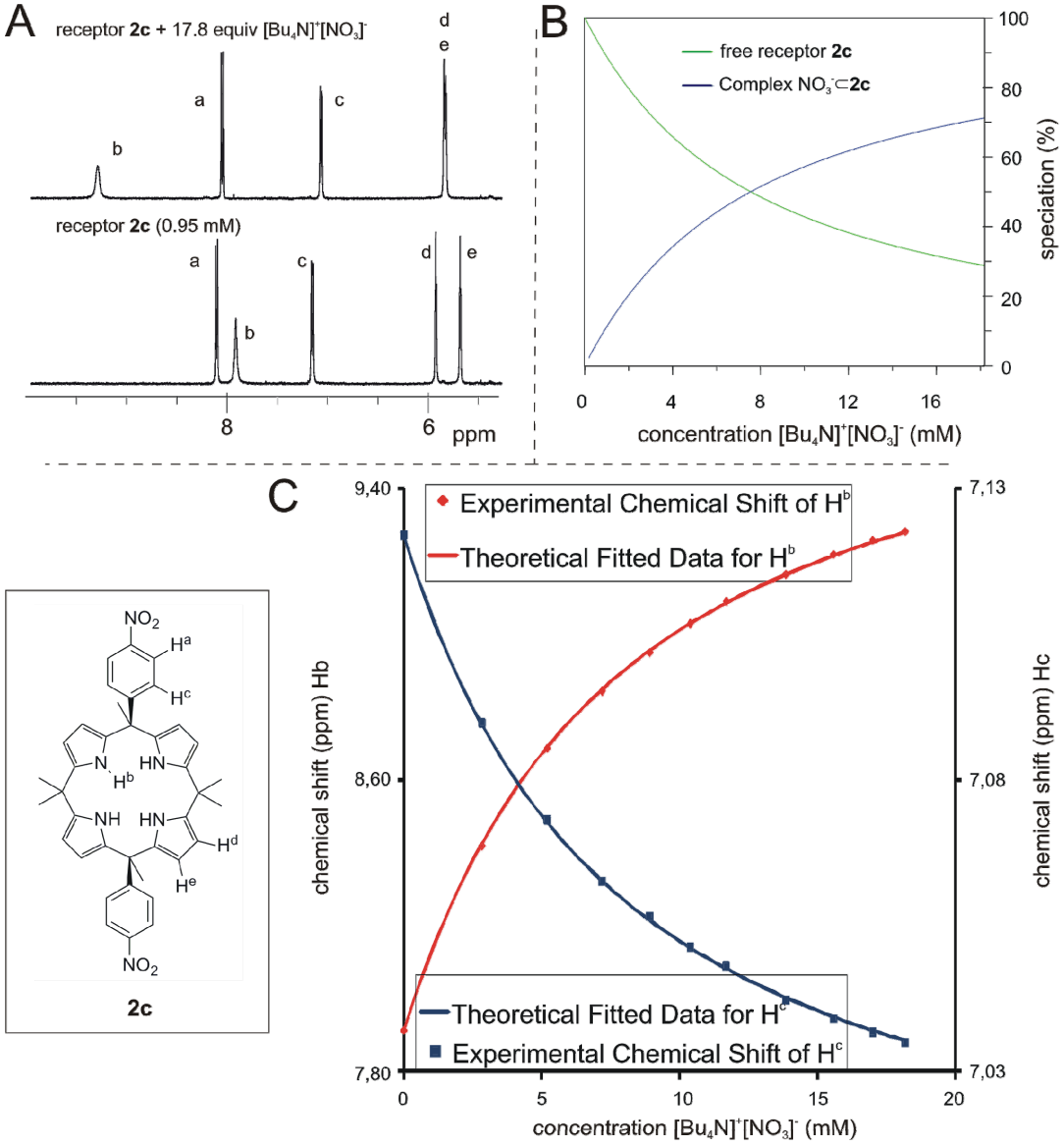


**Figure S 4** Binding data taken from the titration of calixpyrrole **2c** with $[Bu_4N]^+[NO_3]^-$. panel A: $^1$H NMR (500 MHz, $CD_3CN$, 298 K) spectra of the starting point (0.95 mM **2c**) and end point (0.95 mM **2c** with 17.8 equiv $[Bu_4N]^+[NO_3]^-$) of the titration. Panel B: speciation of free calixpyrrole **2c** and host guest complex $NO_3^-\subset$**2c** as a function of $[Bu_4N]^+[NO_3]^-$ concentration. Panel C: fitting of the $^1$H NMR data

**Calixpyrrole 2d nitrate binding**

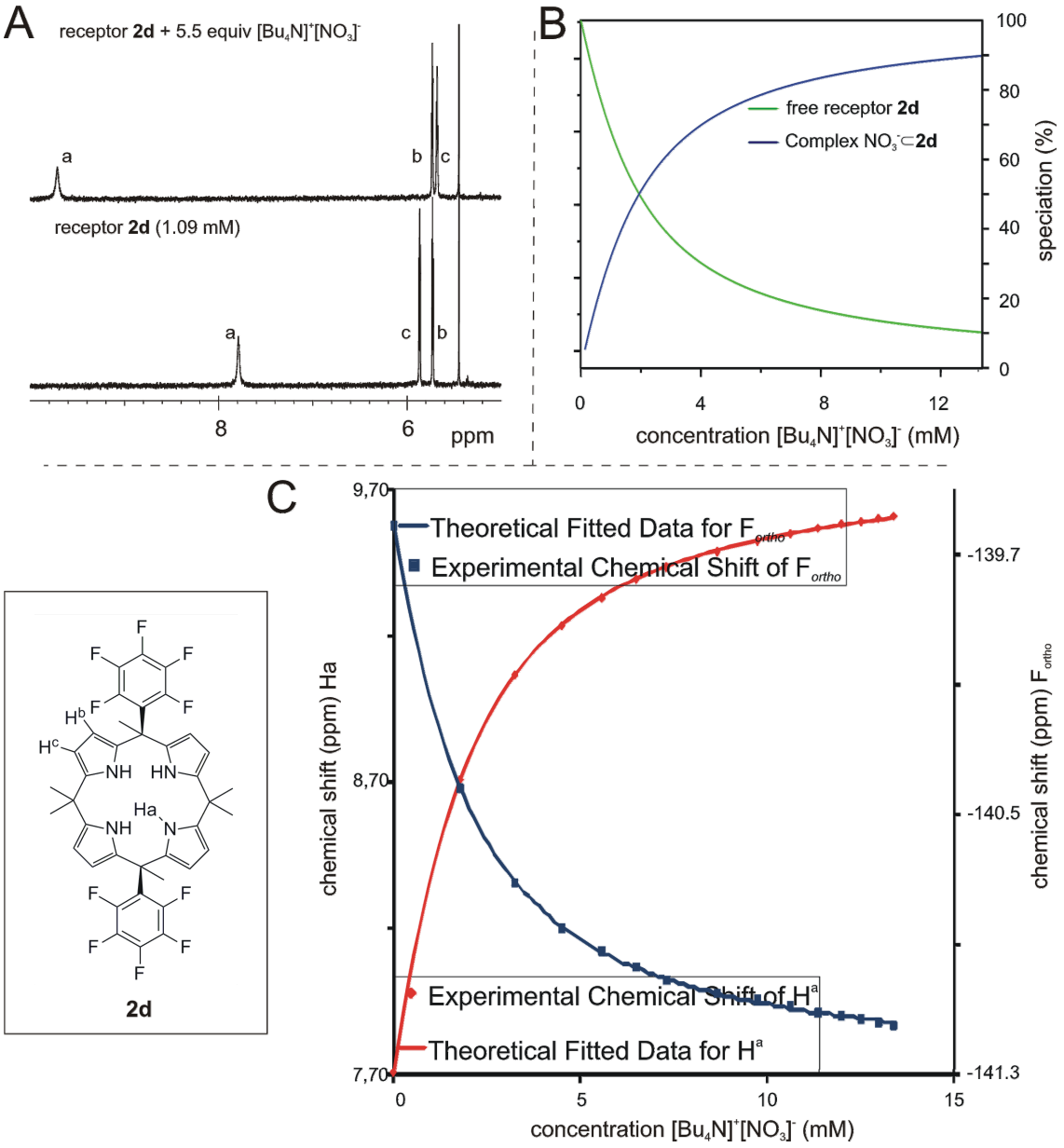


**Figure S 5** Binding data taken from the titration of calixpyrrole **2d** with $[Bu_4N]^+[NO_3]^-$. panel A: $^1$H NMR (400 MHz, $CD_3CN$, 298 K) spectra of the starting point (1.09 mM **2d**) and mid-point (1.09 mM **2d** with 5.5 equiv $[Bu_4N]^+[NO_3]^-$) of the titration. Panel B: speciation of free calixpyrrole **2d** and host guest complex $NO_3^-\subset$**2d** as a function of $[Bu_4N]^+[NO_3]^-$ concentration. Panel C: fitting of the $^1$H NMR data

**Calixpyrrole 2e nitrate binding**

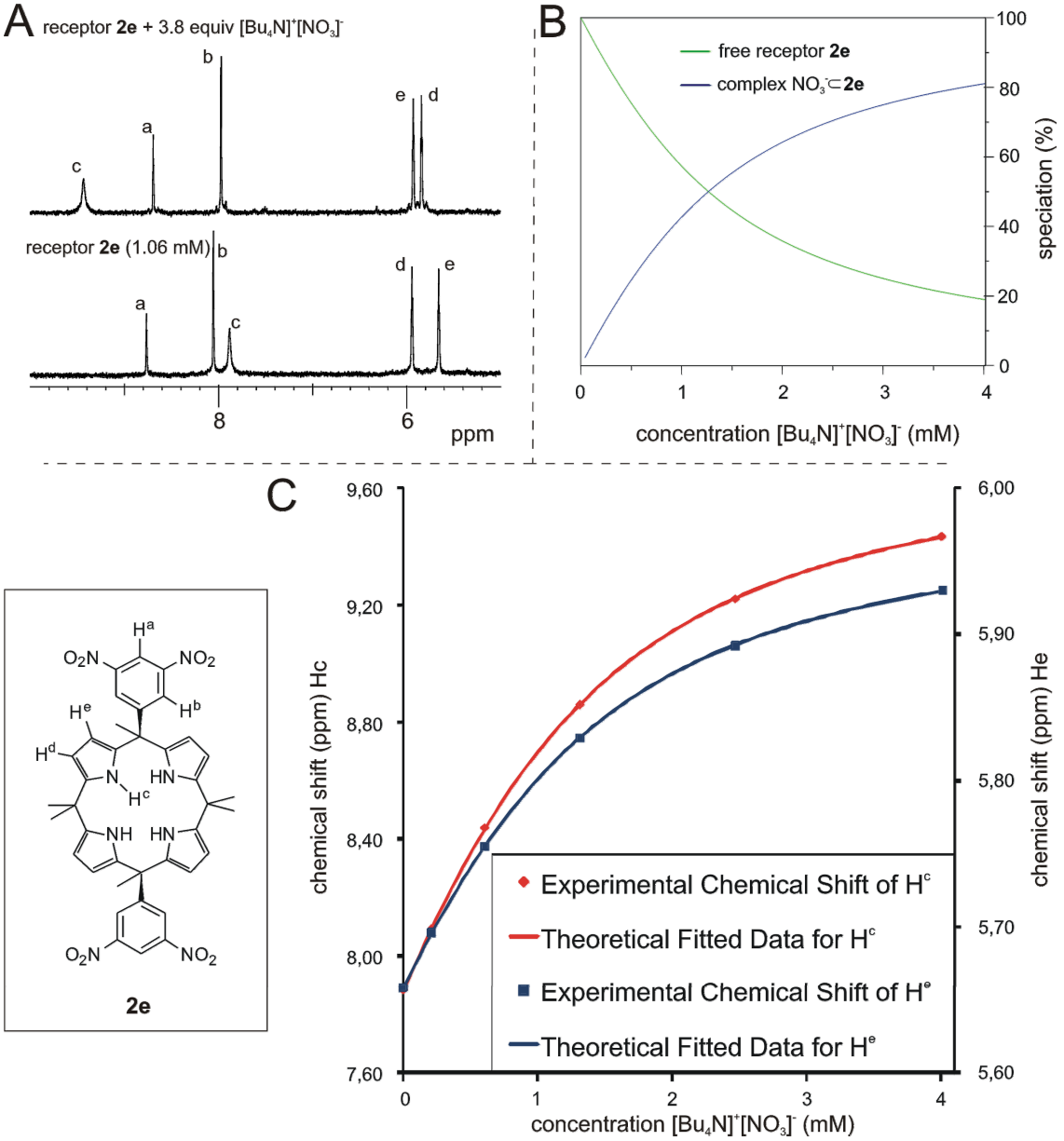


**Figure S 6** Binding data taken from the titration of calixpyrrole **2e** with $[Bu_4N]^+[NO_3]^-$. panel A: $^1$H NMR (400 MHz, $CD_3CN$, 298 K) spectra of the starting point (1.06 mM **2e**) and end point (1.06 mM **2e** with 3.8 equiv $[Bu_4N]^+[NO_3]^-$) of the titration. Panel B: speciation of free calixpyrrole **2e** and host guest complex $NO_3^-\subset$**2e** as a function of $[Bu_4N]^+[NO_3]^-$ concentration. Panel C: fitting of the $^1$H NMR data

**Calixpyrrole 3e nitrate binding**

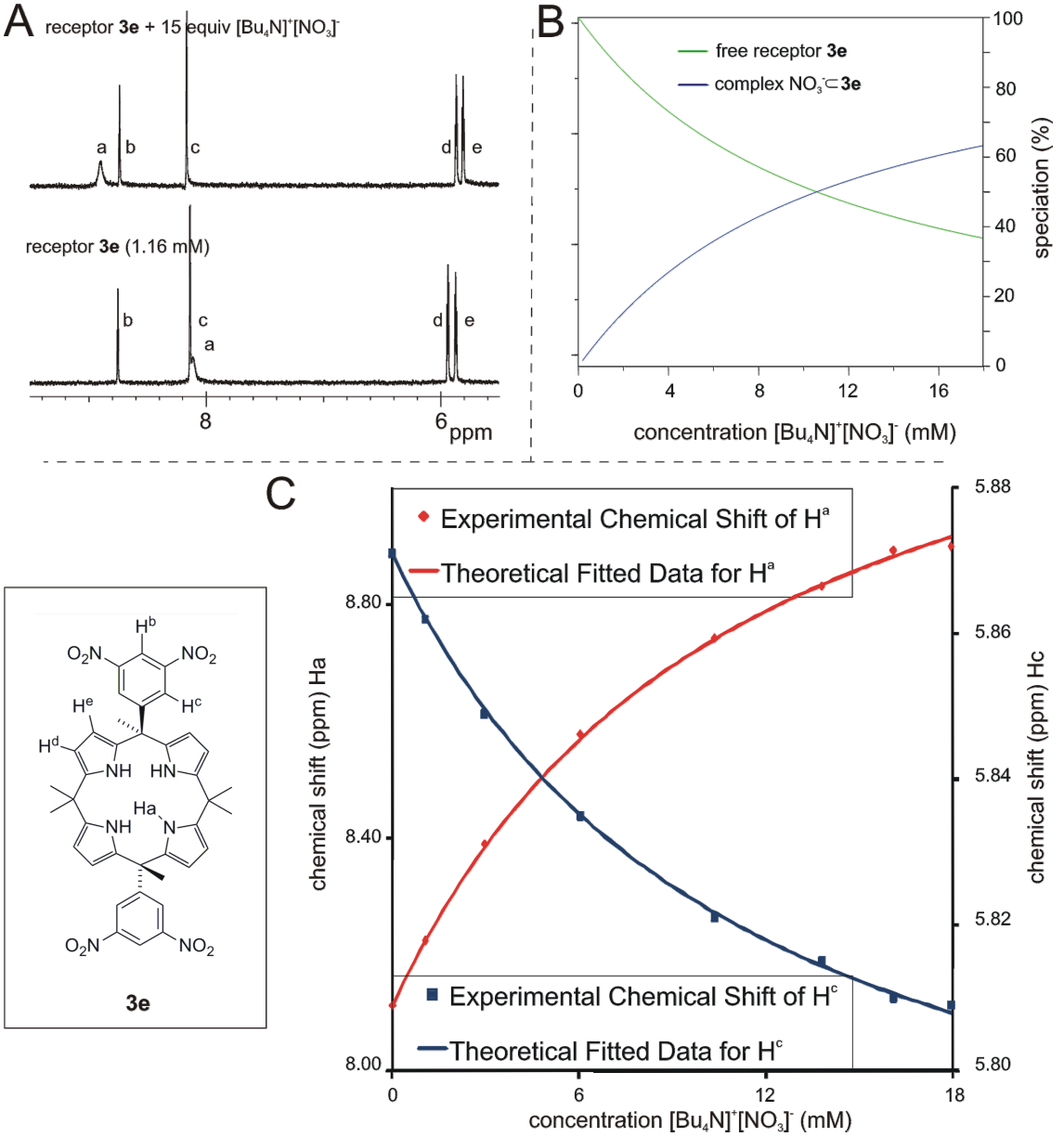


**Figure S 7** Binding data taken from the titration of calixpyrrole **3e** with $[Bu_4N]^+[NO_3]^-$. panel A: $^1$H NMR (400 MHz, $CD_3CN$, 298 K) spectra of the starting point (1.16 mM **3e**) and end point (1.16 mM **3e** with 15 equiv $[Bu_4N]^+[NO_3]^-$) of the titration. Panel B: speciation of free calixpyrrole **3e** and host guest complex $NO_3^-\subset$**3e** as a function of $[Bu_4N]^+[NO_3]^-$ concentration. Panel C: fitting of the $^1$H NMR data

**Alternative x-ray structure of the complex $[Me_4N]^+[NO_3]^-\subset$2e**

Crystals of the complex $[Me_4N]^+[NO_3]^-\subset$**2e** were grown from slow diffusion of acetonitrile into a THF solution of the salt and receptor. X-ray analysis of these crystals showed only one binding geometry.

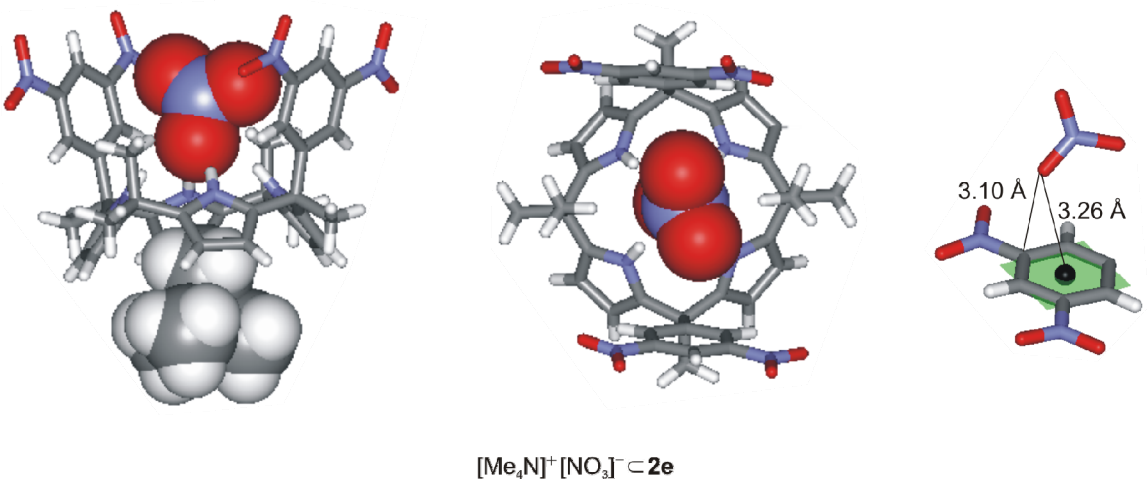


**Figure S 8** Side and top views of the only binding geometry seen in the solid-state structure of the complex $[Me_4N]^+[NO_3]^-\subset$**2e** obtained from crystals grown from a THF solution. The $[Me_4N]^+[NO_3]^-$ contained a small amount of chloride and so in the structure there is a 12% occupancy of chloride in the binding pocket. In this figure chloride has been removed from the structure for purposes of clarity. Furthermore, the structure contains disorder. The nitrate exists in two positions (both perpendicular to the aromatic walls) and the nitro substituents also exist in two positions. This disorder has been removed in the figure. A solvent molecule is omitted for clarity. The $Me_4N^+$ cation is omitted from top view also for clarity. $[Me_4N]^+[NO_3]^-$ is shown in CPK model and **2e** in stick representation.

**p$K_a$ changes of the pyrrole NHs in receptors 2a-2e and the effect on hydrogen bonding**

To gain an understanding of how the different aromatic walls affect the p$K_a$ of the pyrrole NH groups of receptors **2a-e** we calculated the electrostatic potential values at the nitrogen nuclei (EPN) of the corresponding dipyromethanes **S4a**, **S4c** and **S4e**. The calculation of EPN values is a well-known method for the theoretical estimation of p$K_a$s and acidity differences in different categories of compounds.[6,7,8] The calculations were performed on the dipyromethanes and not the calixpyrroles in order to minimize the computational cost of the calculations. Going from **S4a** to **S4c** to **S4e** the values steadily become more positive (a change in EPN of about 12 kcal/mol). This change in EPN values can be roughly related to a decrease of about 2 p$K_a$ units going from **S4a** to **S4e**.[8] Using the p$K_a$ slide rule introduced by Gilli *et. al.* one can obtain a rough idea of the strength of hydrogen bonds based on the p$K_a$ values of the acceptor and donor.[9] If we assume values of about 17 for the p$K_a$ of the pyrrole NHs then a $\Delta$p$K_a$ value of about 18 is obtained in relation to nitrate. That means that according to the slide rule, the strength of hydrogen bonding between calix[4]pyrroles **2** and nitrate will not change appreciably within a $\Delta$p$K_a$ window of 17 to 19. Obviously this is a rough estimation, but it serves to support our claim, also based on $^1$H NMR data, that the primary hydrogen bonding interaction between calix[4]pyrroles and nitrate is not perturbed by the aromatic walls or structural changes to those walls.

# Ion transport

**Table S 1. Summary of transport data[a]**

| entry | Calixpyrrole | HPTS (NaCl) $EC_{50}$ (nM)[b] | HPTS (CsCl) $EC_{50}$ (nM)[b] | CF (NaCl) $EC_{50}$ (nM)[b] | $Cs^+/Na^+$ [c] | $Cl^-/Br^-$ [c] | $NO_3^-/Cl^-$ [c] |
|---|---|---|---|---|---|---|---|
| 1 | **2a** | 350±20 | 9.7±0.4 | 1300±100 | 2.8 | 0.9 | 0.8 |
| 2 | **2b** | 1200±300 | 150±20 | 12900±600 | 2.7 | 0.7 | 1.2 |
| 3 | **2c** | 8.4±0.3 | 7.3±0.3 | 1600±500 | 1.2 | 1.1 | 1.4 |
| 4 | **2d** | 37±4[e] | 2.4±0.2 | 900±200 | 3.8 | 1.7 | 2.1[f] |
| 5 | **2e** | 2.0±0.4 | 0.73±0.06 | 10000±2000 | 1.0 | 1.2 | 1.7 |
| 6 | **1** | 960±300 | 4.5±0.3 | >50000 | Nd | Nd | Nd |
| 7 | **3d** [d] | 110±20[e] | 51±3 | >50000 | 1.3 | 2.0 | 0.1[f] |
| 8 | **3e** | 11.0±1.0 | 7.0±2.0 | >50000 | 0.9 | 1.5 | 0.4 |

[a]For original data, see SI. [b]Effective calix[4]pyrrole concentration needed to reach 50 % activity in the assay. [c]Relative activity in the HPTS assay with different extravesicular ions: external cesium (CsCl) compared with external sodium (NaCl), external chloride (NaCl) compared with external bromide (NaBr), external nitrate ($NaNO_3$) compared with external chloride (NaCl). [d]The α,β-isomer of **2d**. [e]The same trend as with nitrophenyl derivatives **2e**/**3e** was observed, the α,α-isomer **2d** is more active than the α,β-isomer **3d** but with overall weaker activities as compared to the nitro compounds due to the important differences in lipophilicity.[10] [f]The nitrate selectivity is only observed for the α,α-isomer **2d** but not α,β-isomer **3d**. This finding validates the interpretation of the results of the nitro compounds **2e**/**3e**.

## Vesicle Preparation [11,12]

**Vesicle preparation (HPTS)**. A thin lipid film was prepared by evaporating a solution of 25 mg EYPC in 2 ml MeOH/$CHCl_3$ (1:1) on a rotary evaporator (40 °C) and then *in vacuo* overnight. After hydration (> 30 min) with 1.0 ml buffer (100 mM NaCl, 10 mM Hepes, 1 mM HPTS, pH 7.0), the resulting suspension was subjected to >5 freeze-thaw cycles (liquid $N_2$, 37 °C water bath) and >15 times extruded through a polycarbonate membrane (pore size 100 nm, Avanti). Extravesicular components were removed by size exclusion chromatography (Sephadex G-50, Sigma-Aldrich) with 100 mM NaCl, 10 mM Hepes, pH 7.0. Final conditions: ~2.5 mM EYPC; inside: 100 mM NaCl, 10 mM Hepes, 1 mM HPTS, pH 7.0; outside: 100 mM NaCl, 10 mM Hepes, pH 7.0.

Vesicles for the HPTS assay with CsCl were prepared in a similar manner but replacing NaCl by CsCl.

**Vesicle preparation (CF)**. A thin lipid film was prepared by evaporating a solution of 25 mg EYPC in 2 ml MeOH/$CHCl_3$ (1:1) on a rotary evaporator (40 °C) and then *in vacuo* overnight. After hydration (> 30 min) with 1.0 ml buffer (10 mM Hepes, 10 mM NaCl, 50 mM CF, pH 7.0), the resulting suspension was subjected to >5 freeze-thaw cycles (liquid $N_2$, 37 °C water bath), and >15 times extruded through a polycarbonate membrane (pore size 100 nm). Extravesicular components were removed by size exclusion chromatography (Sephadex G-50, Sigma-Aldrich) with 10 mM Hepes, 107 mM NaCl, pH 7.0. Final conditions: ~2.5 mM EYPC; inside: 10 mM Hepes, 10 mM NaCl, 50 mM CF, pH 7.0; outside: 10 mM Hepes, 107 mM NaCl, pH 7.0.

**Determination of transport activity with the HPTS assay.**

In a typical experiment, HPTS⊂EYPC-LUVs (25 µl, final lipid concentration ~30 µM) were added to gently stirred, thermostated buffer (1.950 ml; 100 mM NaCl, 10 mM Hepes, pH 7.0; 25 °C) in a disposable plastic cuvette. Fluorescence emission was followed at $\lambda_{em}$ = 510 nm ($\lambda_{ex}$ = 450 / 405 nm) during the addition of first 0.5 M NaOH (20 µl) and then transporter (20 µl stock solution, in DMSO), and finally excess gramicidin D at the end of the experiment (20 µl, 100 µM in DMSO).

Time courses of fluorescence intensity $I_F$ were obtained by ratiometric analysis ($R = I_{t,450} / I_{t,405}$) and normalization according to equation (1),

$$I_F = \frac{R_t - R_0}{R_\infty - R_0} \qquad (1)$$

where $R_0 = R_t$ right before the addition of transporter and $R_\infty = R_t$ after addition of gramicidin D (Figure S 9 - Figure S 14, left side). $I_F$ at 300 s just before addition of gramicidin D was defined as fractional activity $Y$, and analyzed with the Hill equation (2) to give effective concentration $EC_{50}$ and the Hill coefficient $n$ (Figure S 9 - Figure S 14, right side).

$$Y = Y_\infty + \frac{(Y_0 - Y_\infty)}{1 + \left(\frac{c}{EC_{50}}\right)^n} \qquad (2)$$

where $Y_0$ is $Y$ in absence of transporter, $Y_\infty$ is $Y$ with excess transporter, and $c$ is the transporter concentration in the cuvette.

The HPTS assay with CsCl is similar but using CsCl HPTS⊂EYPC-LUVs vesicles and CsCl buffer solutions.

**Ion transport: HPTS assay (NaCl)**

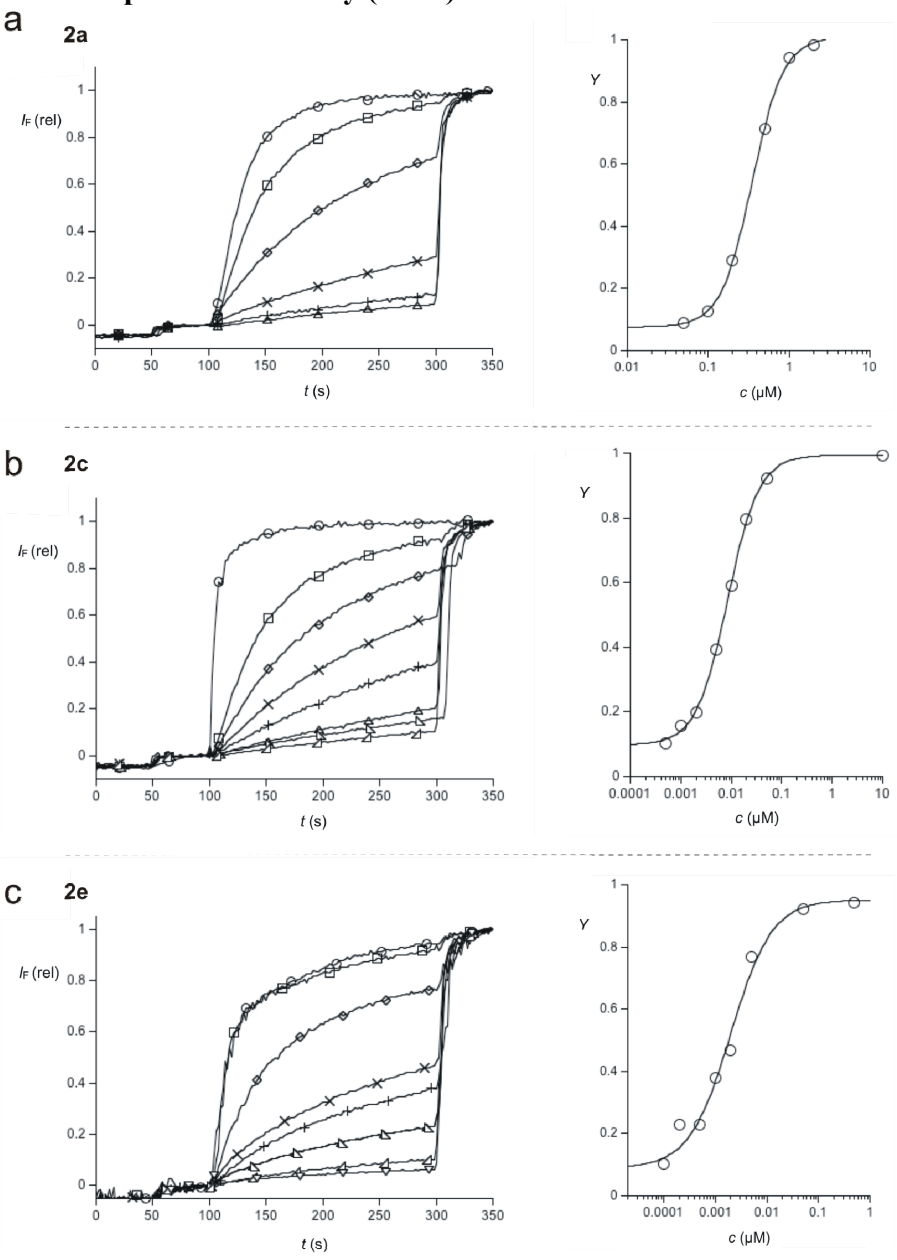


**Figure S 9** (**Left)**: Fluorescence traces for compounds **2a**, **2c** and **2e** in the HPTS assay (NaCl). **a**) Fractional emission $I_F$ during the addition of NaOH (20 µl, 0.5 M, 50 s) then **2a** (with increasing activity: 50 nM (Δ), 100 nM (+), 200 nM (x), 500 nM (◇), 1 µM (□), 2 µM (○), 20 µl, 100 s) and gramicidin D (20 µL, 100 µM, 300 s) to HPTS⊂EYPC-LUVs in NaCl (100 mM, 10 mM Hepes buffer, pH 7). **b**) Same for **2c** (with increasing activity: 500 pM (◿), 1 nM (◺), 2 nM (Δ), 5 nM (+), 10 nM (x), 20 nM (◇), 50 nM (□), 10 µM (○), 20 µl, 100 s).**c**) Same for **2e** (with increasing activity: 0 pM (▽), 100 pM (◿), 200 pM (◺), 500 pM (Δ), 1 nM (+), 2 nM (x), 5 nM (◇), 50 nM (□), 500 nM (○), 20 µl, 100 s). (**Right)**: Dose response curves for compounds **a**) **2a**, **b**) **2c**, **c**) **2e** in the HPTS assay.

**Ion transport: HPTS assay (NaCl)**

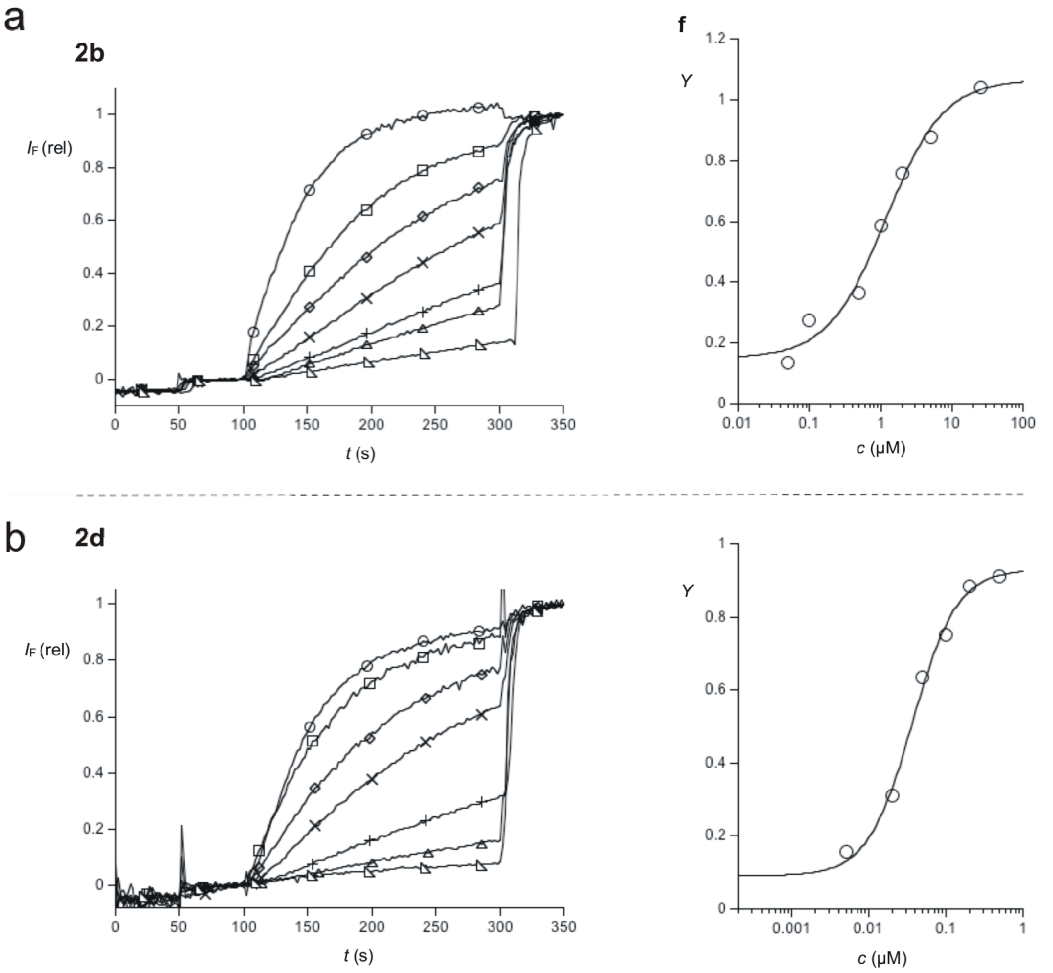


**Figure S 10** (**Left)**: Fluorescence traces for compounds **2b** and **2d** in the HPTS assay (NaCl). **a**) Fractional emission $I_F$ during the addition of NaOH (20 µl, 0.5 M, 50 s) then **2b** (with increasing activity: 50 nM (◺), 100 nM (Δ), 500 nM (+), 1 µM (x), 2 µM (◇), 5 µM (□), 25 µM (◯), 20 µl, 100 s) and gramicidin D (20 µL, 100 µM, 300 s) to HPTS⊂EYPC-LUVs in NaCl (100 mM, 10 mM Hepes buffer, pH 7). **b**) Same for **2d** (with increasing activity: 0 µM (◺), 5 nM (Δ), 20 nM (+), 50 nM (x), 100 nM (◇), 200 nM (□), 500 nM (◯), 20 µl, 100 s). (**Right)**: Dose response curves for compounds **a**) **2b**, **b**) **2d** in the HPTS assay.

**Ion transport: HPTS assay (NaCl)**

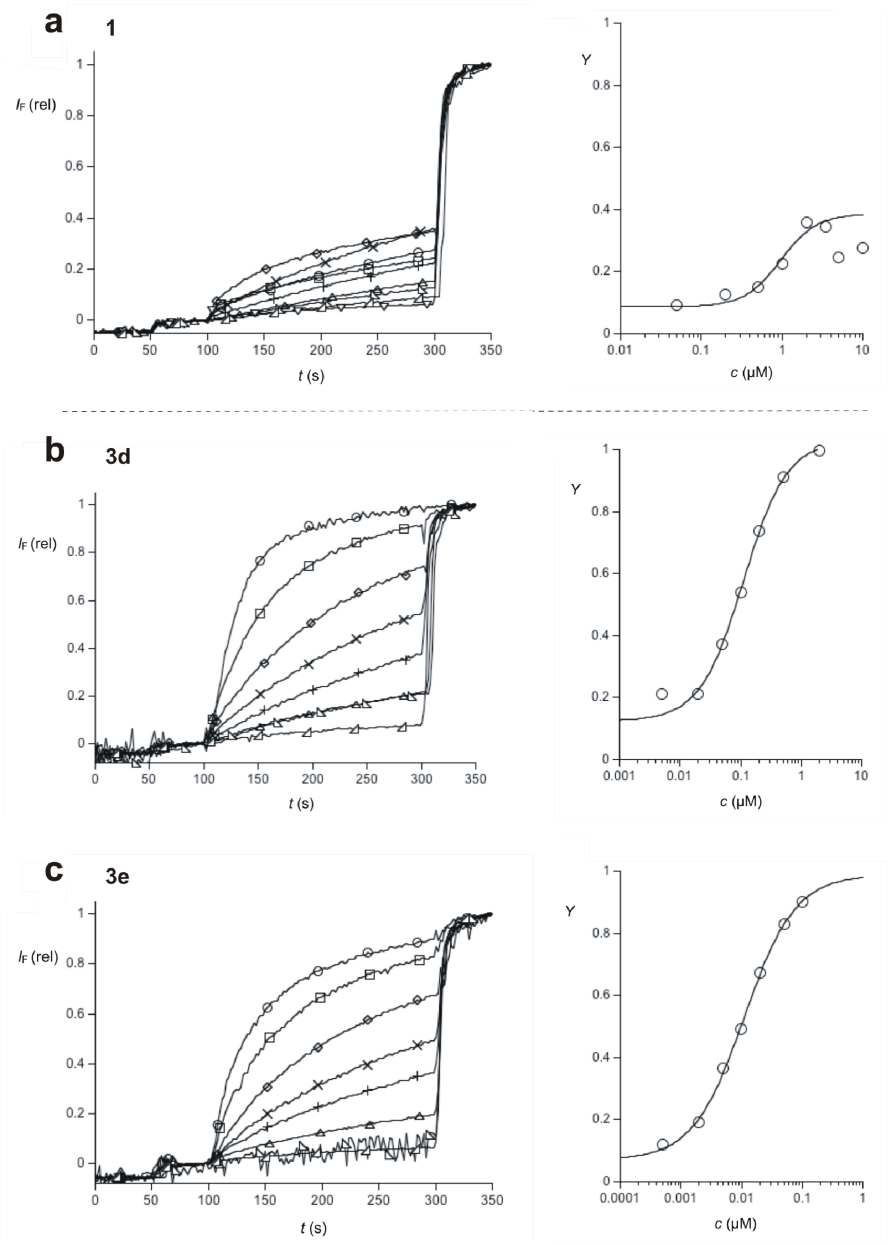


**Figure S 11 (Left)**: Fluorescence traces for compounds **1 3d** and **3e** in the HPTS assay (NaCl). **a**) Fractional emission $I_F$ during the addition of NaOH (20 µl, 0.5 M, 50 s) then **1** (with increasing activity: 0 nM (▽), 50 nM (◿), 200 nM (◺), 500 nM (Δ), 1 µM (+), 2 µM (x), 3.5 µM (◇), 5 µM (□), 10 µM (◯), 20 µl, 100 s) and gramicidin D (20 µL, 100 µM, 300 s) to HPTS⊂EYPC-LUVs in NaCl (100 mM, 10 mM Hepes buffer, pH 7). **b**) Same for **3d** (with increasing activity: 0 nM (◿), 5 nM (◿), 20 nM (Δ), 50 nM (+), 100 nM (x), 200 nM (◇), 500 nM (□), 2 µM (◯), 20 µl, 100 s) **c**) Same for **3e** (with increasing activity: 0 pM (◿), 500 pM (◺), 2 nM (Δ), 5 nM (+), 10 nM (x), 20 nM (◇), 50 nM (□), 100 nM (◯), 20 µl, 100 s). **(Right)**: Dose response curves for compounds **a**) **1** and **b**) **3d** and **c**) **3e** in the HPTS assay.

**Ion transport: HPTS assay (CsCl)**

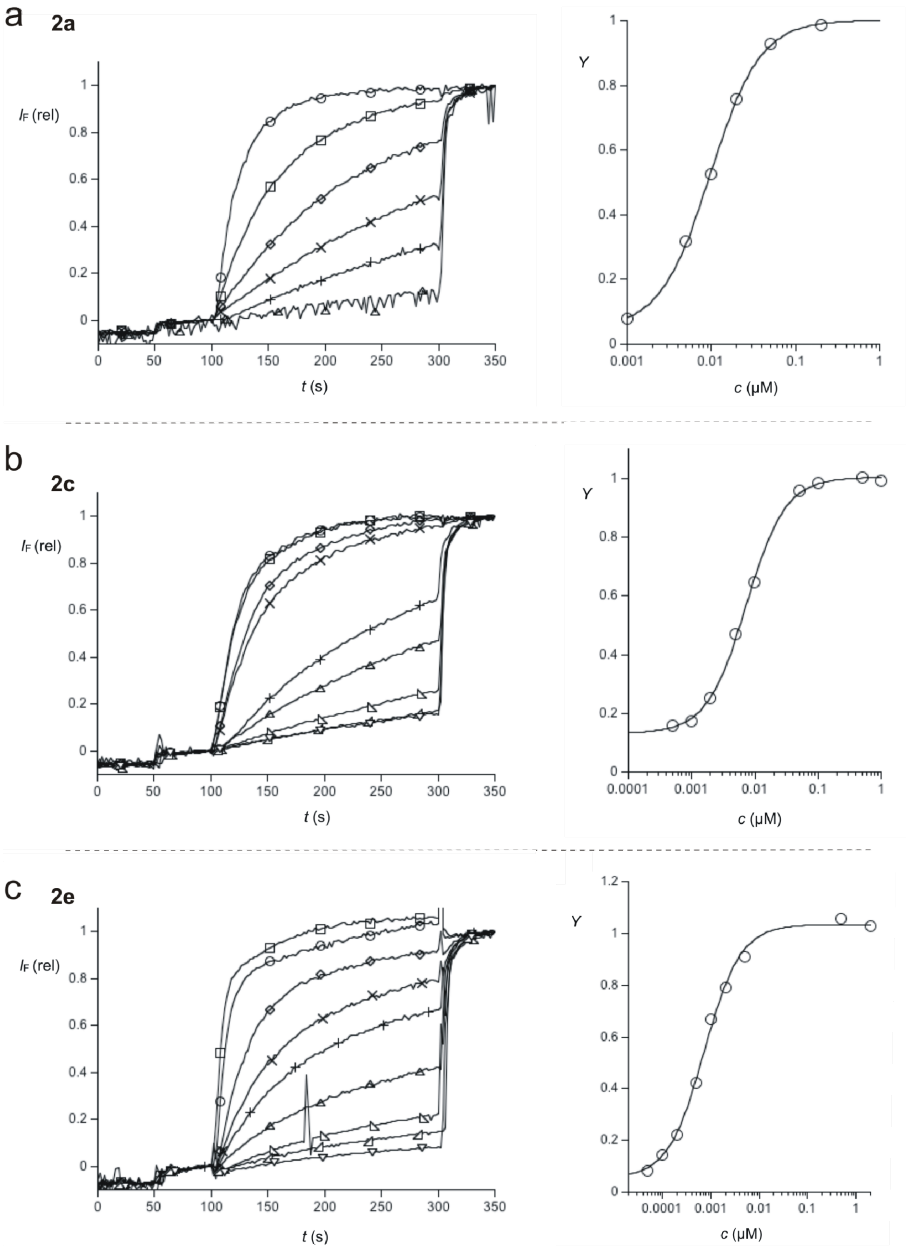


**Figure S 12 (Left)**: Fluorescence traces for compounds **2a**, **2c** and **2e** in the HPTS assay (CsCl). **a**) Fractional emission $I_F$ during the addition of NaOH (20 µl, 0.5 M, 50 s) then **2a** (with increasing activity: 1 nM (Δ), 5 nM (+), 10 nM (x), 20 nM (◇), 50 nM (□), 200 nM (○), 20 µl, 100 s) and gramicidin D (20 µL, 100 µM, 300 s) to HPTS⊂EYPC-LUVs in CsCl (100 mM, 10 mM Hepes buffer, pH 7). **b**) Same for **2c** (with increasing activity: 500 pM (▽), 1 nM (◿), 2 nM (◺), 5 nM (Δ), 10 nM (+), 50 nM (x), 100 nM (◇), 500 nM (□), 1 µM (○), 20 µl, 100 s). **c**) Same for **2e** (with increasing activity: 50 pM (▽), 100 pM (◿), 200 pM (◺), 500 pM (Δ), 1 nM (+), 2 nM (x), 5 nM (◇), 500 nM (□), 2 µM (○), 20 µl, 100 s). (**Right)**: Dose response curves for compounds **a**) **2a**, **b**) **2c**, **c**) **2e** in the HPTS assay.

**Ion transport: HPTS assay (CsCl)**

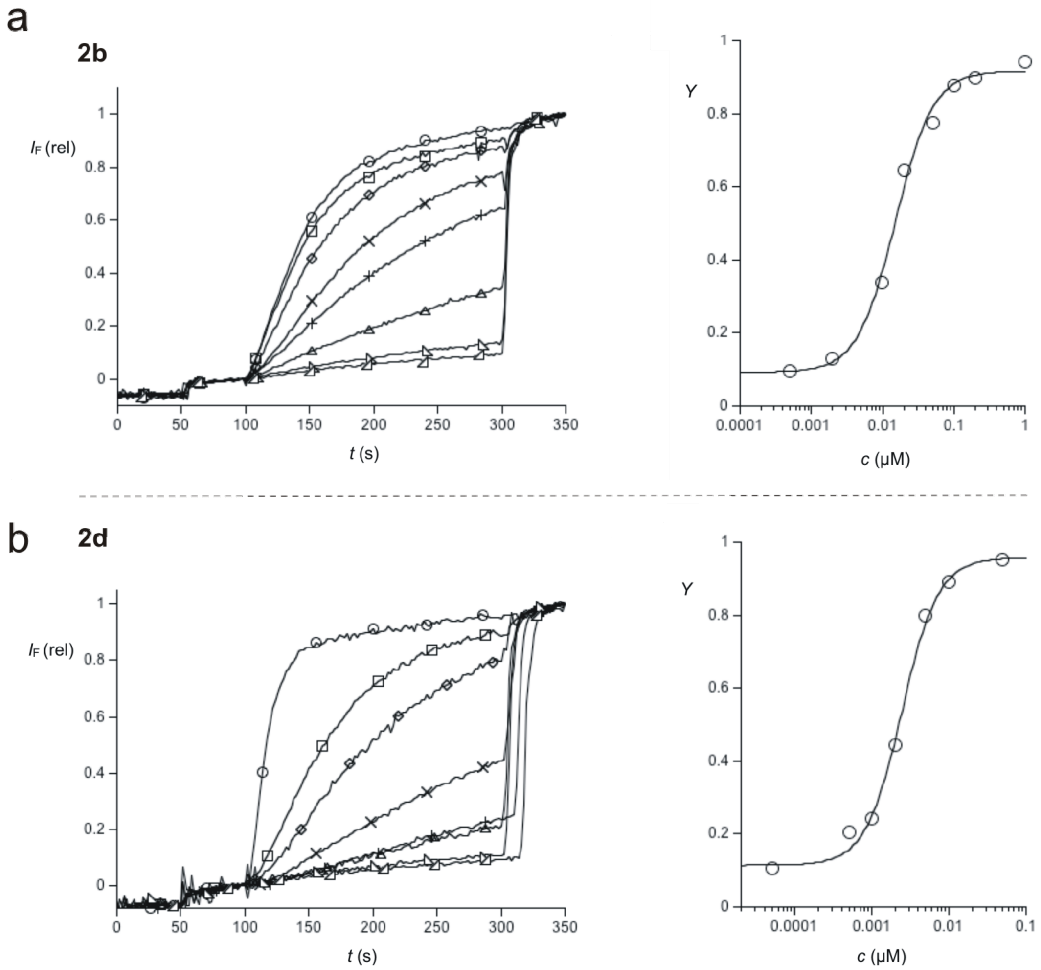


**Figure S 13 (Left)**: Fluorescence traces for compounds **2b** and **2d** in the HPTS assay (CsCl). **a**) Fractional emission $I_F$ during the addition of NaOH (20 µl, 0.5 M, 50 s) then **2b** (with increasing activity: 500 pM (◿), 2 nM (◺), 10 nM (Δ), 20 nM (+), 50 nM (x), 100 nM (◇), 200 nM (□), 1 µM (◯), 20 µl, 100 s) and gramicidin D (20 µL, 100 µM, 300 s) to HPTS⊂EYPC-LUVs in CsCl (100 mM, 10 mM Hepes buffer, pH 7). **b**) Same for **2d** (with increasing activity: 0 nM (◿), 0.05 nM (◺), 0.5 nM (Δ), 1 nM (+), 2 nM (x), 5 nM (◇), 10 nM (□), 50 nM (◯), 20 µl, 100 s). **(Right)**: Dose response curves for compounds **a**) **2b** and **b**) **2d** in the HPTS assay.

**Ion transport: HPTS assay (CsCl)**

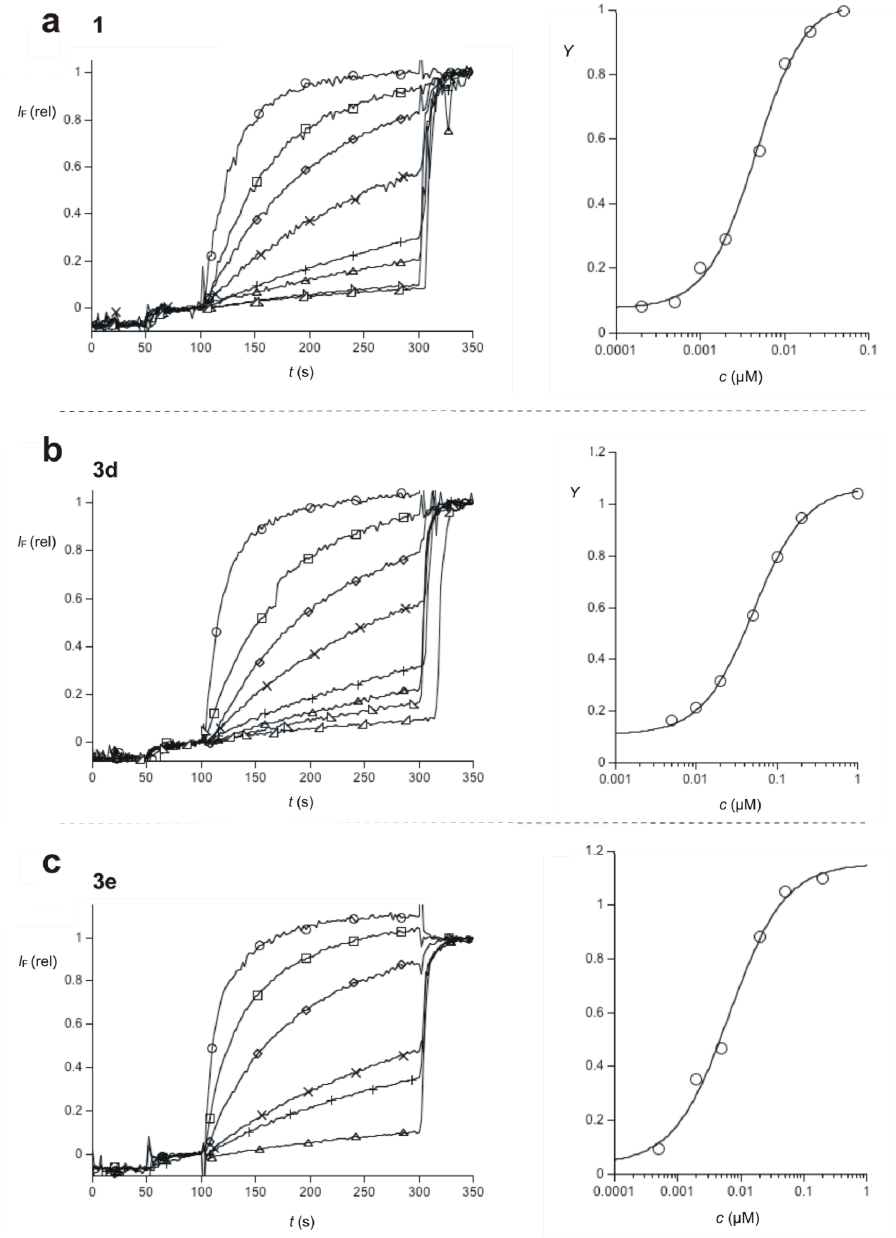


**Figure S 14 (Left)**: Fluorescence traces for compounds **1 3d** and **3e** in the HPTS assay (CsCl). **a**) Fractional emission $I_F$ during the addition of NaOH (20 µl, 0.5 M, 50 s) then **1** (with increasing activity: 200 pM (◿), 500 pM (◺), 1 nM (Δ), 2 nM (+), 5 nM (x), 10 nM (◇), 25 nM (□), 50 nM (◯), 20 µl, 100 s) and gramicidin D (20 µL, 100 µM, 300 s) to HPTS⊂EYPC-LUVs in CsCl (100 mM, 10 mM Hepes buffer, pH 7). **b**) Same for **3d** (with increasing activity: 0 nM (◿), 5 nM (◺), 10 nM (Δ), 20 nM (+), 50 nM (x), 100 nM (◇),200 nM (□), 1 µM (◯), 20 µl, 100 s) **c**) Same for **3e** (with increasing activity: 500 pM (Δ), 2 nM (+), 5 nM (x), 20 nM (◇), 50 nM (□), 200 nM (◯), 20 µl, 100 s). **(Right)**: Dose response curves for compounds **a**) **1 b**) **3d** and **c**) **3e** in the HPTS assay.

**Non-specific leakage: CF assay**

All the compounds were tested for membrane "imperfections" or membrane disruption upon the addition of the studied compounds. The typical assay to test for membrane leakage, rather than membrane transport, is the carboxyfluorescein (CF) assay.[12] In this assay, CF at a self-quenched concentration is confined inside LUVs which are then dispersed in an isoosmotic buffer. The potential transporter is added and upon disruption of the membrane the fluorescence increases due to the released CF from the vesicles.

In a typical experiment, CF⊂EYPC-LUVs (25 µl, inside: 10 mM Hepes, 10 mM NaCl, 50 mM CF, pH 7.0) were added to 1975 µl gently stirred, thermostated buffer (10 mM Hepes, 100 mM NaCl, pH 7.0) in a disposable plastic cuvette. The time-dependent changes in fluorescence intensity $I_t$ ($\lambda_{exc}$ = 492 nm, $\lambda_{em}$ = 517 nm) were monitored during the addition of the studied calix[4]pyrroles (**1**, **2a-e** and **3d**,**e** in DMSO; 50 s) and addition of triton X-100 (40 µl 1.2 % aq; 250 s). Time courses of $I_t$ were normalized to fractional intensities $I_F$ using equation (3).

$$I_F = (I_t - I_0) / (I_\infty - I_0) \qquad (3)$$

where $I_0 = I_t$ before calix[4]pyrrole addition and $I_\infty = I_t$ after lysis (Figure S 15 and Figure S 16, left). $I_F$ at 250 s after the start of the experiment just before lysis was defined as transmembrane activity Y, and Hill analysis was applied to determine $EC_{50}$ values (Figure S 15 and Figure S 16, right).

For all the compounds tested, the $EC_{50}$ value for the CF assay was significantly higher than the $EC_{50}$ value for the HPTS assay, thus, confirming that the observed trends come from ion transport rather than leakage.

It is to be noted that the compounds containing the stronger anion-π donor also show the best ratios between activity and leakage. This is not necessarily due to a better compatibility of the anion-π systems with the membrane but rather the consequence of a significantly higher activity towards anion transport as shown by the fact that the $EC_{50}$ values in the CF assay for "similar" molecules are comparable independently of the nature of their aromatic walls.

**Non-specific leakage: CF assay**

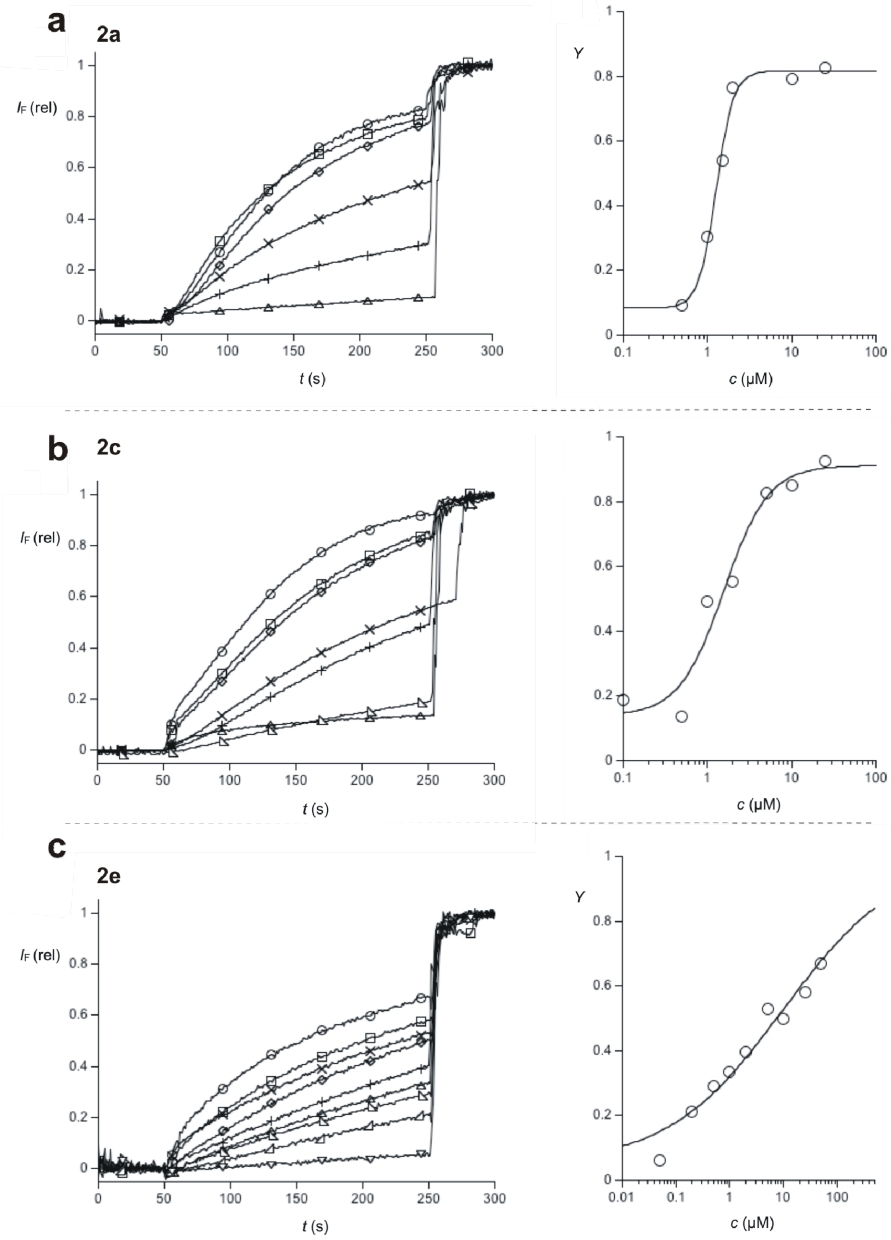


**Figure S 15 (Left)**: Fluorescence traces for compounds **2a**, **2c** and **2e** in the CF assay. **a**) Fluorescence emission during the addition of **2a** (with increasing activity: 500 nM (Δ), 1 μM (+), 1.5 μM (x), 2 μM (◇), 10 μM (□), 20 μM (○), 20 μl, 50 s) and triton X-100 (40 μL, 1.2 %, 250 s) to CF⊂EYPC-LUVs in NaCl (100 mM, 10 mM Hepes buffer, pH 7). **b**) Same for **2c** (with increasing activity: 100 nM (◺), 500 nM (Δ), 1 μM (+), 2 μM (x), 5 μM (◇), 10 μM (□), 25 μM (○), 20 μl, 100 s). **c**) Same for **2e** (with increasing activity: 50 nM (▽), 200 nM (◿), 500 nM (◺), 1 μM nM (Δ), 2 μM (+), 5 μM (x), 10 μM (◇), 25 μM (□), 50 μM (○), 20 μl, 100 s). **(Right)**: Dose response curves for compounds **a**) **2a**, **b**) **2c**, **c**) **2e** in the CF assay.

**Non-specific leakage: CF assay**

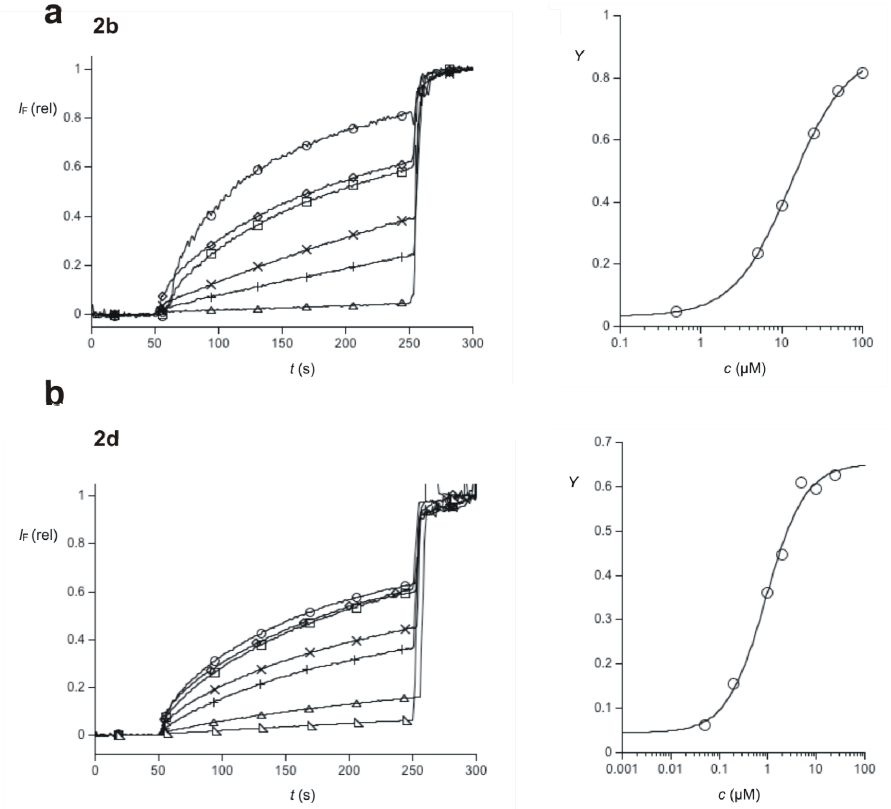


**Figure S 16 (Left)**: Fluorescence traces for compounds **2b** and **2d** in the CF assay. **a**) Fluorescence emission during the addition of **2b** (with increasing activity: 500 nM (Δ), 5 μM (+), 10 μM (x), 25 μM (◇), 50 μM (□), 100 μM (○), 20 μl, 100 s) and triton X-100 (40 μL, 1.2 %, 250 s) to CF⊂EYPC-LUVs in NaCl (100 mM, 10 mM Hepes buffer, pH 7). b) same for **2d** (with increasing activity: 50 nM (◺), 200 nM (Δ), 1 μM (+), 2 μM (x), 5 μM (◇), 10 μM (□), 25 μM (○), 20 μl, 50 s) **(Right)**: Dose response curves for compound **a**) **2b** and **b**) **2d** in the CF assay.

**Ion selectivity in the HPTS assay**

Following established procedures,[12] HPTS⊂EYPC-LUVs (25 µl) prepared as described above were added to 1950 µl gently stirred, thermostated (25 °C) buffer (100 mM $M^+Cl^-$ ($M^+ = Li^+, Na^+, K^+, Rb^+, Cs^+$) or $Na^+X^-$ ($X^- = F^-, OAc^-, Cl^-, Br^-, NO_3^-, I^-, ClO_4^-$), 10 mM Hepes, (pH 7.0) in a disposable plastic cuvette. The time-dependent change in fluorescence intensity was monitored and analyzed as described before to obtain the fractional transmembrane activity *Y* dependent on the externally added cation or anion $M^+X^-$ at a fixed concentration ($EC_{50}$) of transporters. The fractional activity *Y* for NaCl was normalized to 1. Fractional activities are plotted as a function of the anion dehydration energies (Figure S 17 and Figure S 18).

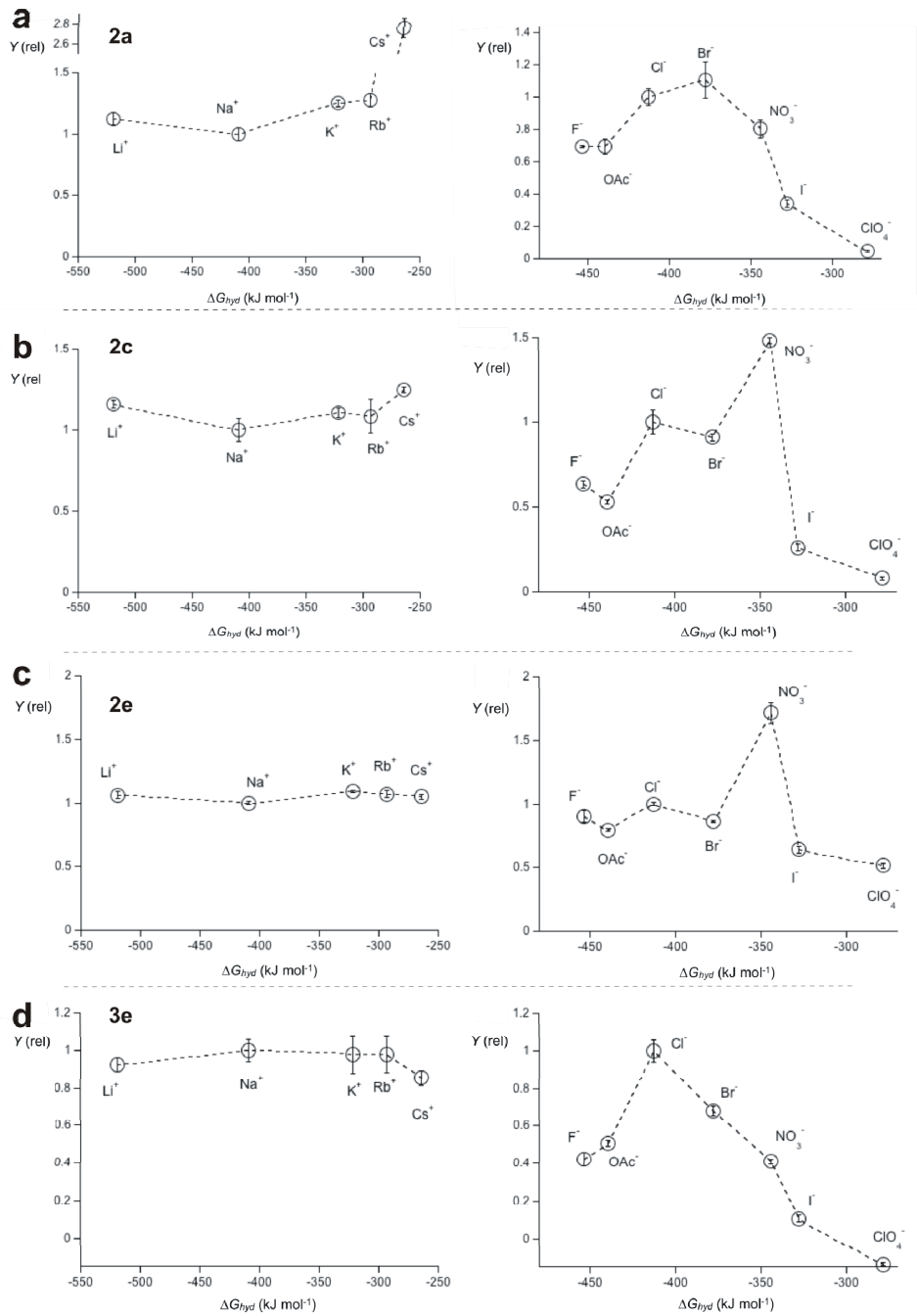


**Figure S 17** Cation and anion selectivity for compounds **2a** (**a**), **2c** (**b**) **2e** (**c**) and **3e** (**d**). **(Left):** Cation selectivity in the HPTS assay as described above (buffer: 100 mM $M^+Cl^-$ ($M^+ = Li^+$, $Na^+$, $K^+$, $Rb^+$, $Cs^+$, 10 mM Hepes, pH 7.0)). **(Right):** Same for anions (buffer: 100 mM $Na^+X^-$ ($X^- = F^-$, $OAc^-$, $Cl^-$, $Br^-$, $NO_3^-$, $I^-$, $ClO_4^-$, 10 mM Hepes,) pH 7.0). The fractional activity *Y* for NaCl is normalized to 1.

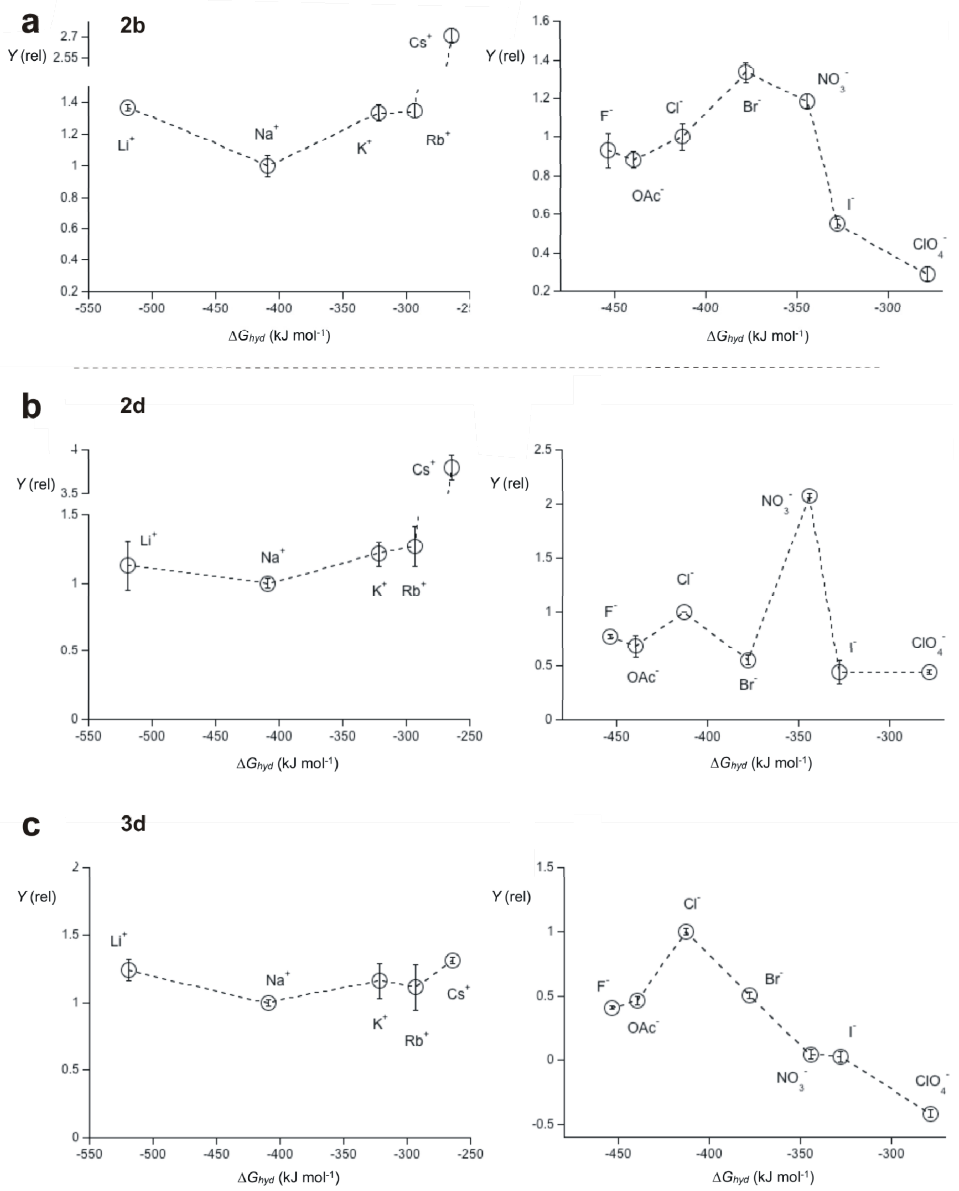


**Figure S 18** Cation and anion selectivity for compounds **2b** (**a**) and **2d** (**b**) and **3d** (**c**). **(Left):** Cation selectivity in the HPTS assay as described above (buffer: 100 mM $M^+Cl^-$ ($M^+$ = $Li^+$, $Na^+$, $K^+$, $Rb^+$, $Cs^+$, 10 mM Hepes, pH 7.0)). **(Right):** Same for anions (buffer: 100 mM $Na^+X^-$ ($X^-$ = $F^-$, $OAc^-$, $Cl^-$, $Br^-$, $NO_3^-$, $I^-$, $ClO_4^-$, 10 mM Hepes,) pH 7.0). The fractional activity *Y* for NaCl is normalized to 1. Notice the nitrate selectivity is only observed with the α,α-isomer **2d** as compared to the α,β-isomer **3d**.

## References


[1] Rothemund, P.; Gage, C. L. *J. Am. Chem. Soc.* **1955**, *77*, 3340.
[2] Bruno, G.; Cafeo, G.; Kohnke, F. H.; Nicolo, F. *Tetrahedron* **2007**, *63*, 10003.
[3] Park, J. S.; Yoon, K. Y.; Kim, D. S.; Lynch, V. M.; Bielawski, C. W.; Johnston, K. P.; Sessler, J. L. *Proc. Natl. Acad. Sci. USA* **2011**, *108*, 20913.
[4] Sobral, A. J. F. N.; Rebanda, N. G. C. L.; da Silva, M.; Lampreia, S. H.; Silva, M. R. *Tetrahedron Lett.* **2003**, *44*, 3971.
[5] HypNMR 2008 Version 4.0.66. Protonic Software. peter.gans@hyperquad.co.uk.
[6] Dimitrova, V.; Ilieva, S.; Galabov, B. *J. Phys. Chem. A* **2002**, *106*, 11801
[7] Galabov, B.; Bobadova-Parvanova, P. *J. Phys. Chem. A* **1999**, *103*, 6793
[8] Liu, S. B.; Pedersen, L. G. *J. Phys. Chem. A* **2009**, *113*, 3648
[9] Gilli, P.; Pretto, L.; Bertolasi, V.; Gilli, G. *Acc. Chem. Res.* **2009**, *42*, 33
[10] Saggiomo, V.; Otto, S.; Marques, I.; Felix, V.; Torroba, T.; Quesada, R. *Chem. Commun.* **2012**, *48*, 5274.
[11] Dawson, R. E.; Hennig, A.; Weimann, D. P.; Emery, D.; Ravikumar, V.; Montenegro, J.; Takeuchi, T.; Gabutti, S.; Mayor, M.; Mareda, J.; Schalley, C. A.; Matile, S. *Nature Chem.* **2010**, *2*, 533.
[12] Matile, S.; Sakai, N. The Characterization of Synthetic Ion Channels and Pores. In *Analytical Methods in Supramolecular Chemistry*; *2nd Edition*, Schalley, C. A., Ed.; Wiley: Weinheim, **2012**, 711-742.